FULL PAPER

Dalton
www.rsc.org/dalton

Preparation and characterization of diarylphosphazene and diarylphosphinohydrazide complexes of titanium, tungsten and ruthenium and phosphorylketimido complexes of rhenium

Andrew R. Cowley, Jonathan R. Dilworth,* Alison K. Nairn and Alasdair J. Robbie
Chemistry Research Laboratory, University of Oxford, 12 Mansfield Road, Oxford, UK OX1 3TA. E-mail: jon.dilworth@chem.ox.ac.uk; Fax: 01865-272690; Tel: 01865-285151

Received 9th November 2004, Accepted 15th December 2004
First published as an Advance Article on the web 24th January 2005

Reaction of the proligand $Ph_2PN(SiMe_3)_2$ (L^1) with WCl_6 gives the oligomeric phosphazene complex $[WCl_4(NPPh_2)]_n$, **1** and subsequent reaction with PMe_2Ph or NBu_4Cl gives $[WCl_4(NPPh_2)(PMe_2Ph)]$ (**2**) or $[WCl_5(NPPh_2)][NBu_4]$ (**3**), respectively. DF calculations on $[WCl_5(NPPh_2)][NBu_4]$ show a W=N double bond (1.756 Å) and a P–N bond distance of 1.701 Å, which combined with the geometry about the P atom suggests, there is no P–N multiple bonding. Reaction of L^1 with $[ReOX_3(PPh_3)_2]$ in MeCN (X = Cl or Br) gives $[ReX_2(NC(CH_3)P(O)Ph_2)(MeCN)(PPh_3)]$ (X = Cl, **4**, X = Br, **5**) which contains the new phosphorylketimido ligand. It is bound to the rhenium centre with a virtually linear Re–N–C arrangement (Re–N–C angle = 176.6°. when X = Cl) and there is multiple bonding between Re and N (Re–N = 1.809(7) Å when X = Cl). The proligand $Ph_2PNHNMe_2$ (L^2H) reacts with $[(C_5H_5)TiCl_3]$ to give $[(C_5H_5)TiCl_2(Me_2NNPPh_2)]$ (**6**). An X-ray crystal structure of the complex shows the ligand (L^2) is bound by both nitrogen atoms. Reaction of the proligands Ph_2PNHNR_2 [R_2 = Me_2 (L^2H), $–(CH_2CH_2)_2NCH_3$ (L^3H), $(CH_2CH_2)_2CH_2$ (L^4H)] with $[\{RuCl(\mu\text{-}Cl)(\eta^6\text{-}p\text{-}MeC_6H_4{}^iPr)\}_2]$ gave $[RuCl_2(\eta^6\text{-}p\text{-}MeC_6H_4{}^iPr)(L)]$ {L = L^2H (**7**), L^3H (**8**), L^4H (**9**)}. The X-ray crystal structures of **7–9** confirmed that the phosphinohydrazine ligand is neutral and bound *via* the phosphorus only. Reaction of complexes **7–9** with $AgBF_4$ resulted in chloride ion abstraction and the formation of the cationic species $[RuCl(\eta^6\text{-}p\text{-}MeC_6H_4{}^iPr)(L)]^+BF_4^-$ {(L = L^2H (**10**), L^3H (**11**), L^4H (**12**)}. Finally, reaction of complex **6** with $[\{RuCl(\mu\text{-}Cl)(\eta^6\text{-}p\text{-}MeC_6H_4{}^iPr)\}_2]$ gave the binuclear species $[(\eta^6\text{-}p\text{-}MeC_6H_4{}^iPr)Cl_2Ru(\mu^2,\eta^3\text{-}Ph_2PNNMe_2)TiCl_2(C_5H_5)]$, **13**.

Introduction

The chemistry of metal complexes which contain metal–nitrogen multiple bonds has been very comprehensively studied.[1–3] The drive to study these complexes comes from a desire to understand the mechanism by which the nitrogenase enzymes operate, for which the key intermediates in the conversion of coordinated N_2 to ammonia are the diazenido (M=N=NH), isodiazene (M≡N–NH_2) and the hydrazido(1−) (M–NH–NH_2) species.[4,5] These types of metal complex have a rich and diverse chemistry in their own right; they show a wide range of different binding modes with a large number of different metals.

In stark contrast to the many M–N–N species known, there are very few examples of complexes containing coordinated N–P(III) ligands, and in almost all of these examples the ligand is bound in neutral form to the metal *via* phosphorus only. Many of these examples incorporate ligands of the type $NHR^1–PR^2{}_2$.[6–10] For example, the Mo complex in which R^1 = H and R^2 = Ph has the molecular structure $[Mo(CO)_4(PPh_2NH_2)_2]$, containing two $H_2N–PPh_2$ ligands bound *trans* to each other *via* phosphorus.[11] This is in contrast to P(V)–N systems, for which there are many examples of complexes containing the M–N–P unit. Roesky *et al.* have prepared the complex, $[TiCl_2(py)_3(NP(S)Ph_2)]$ which incorporates the Ti=N–P(S)Ph_2 unit,[12] and the complex $[(C_5H_5)TiCl_2(NPPh_3)]$ was prepared by Dilworth *et al.*[13,14] Ti complexes with this ligand type have seen recent applications as very effective olefin polymerisation catalysts,[15,16] and there are other examples of Ph_3P–N complexes with metals such as V, Mo and W.

The chemistry of P(III)-containing analogues of hydrazido(1−) complexes (phosphaneazenides) has also been comparatively little explored. Work by Fenske *et al.*[17] involved the use of $[Ph_2P–NPh]^-Li^+$, which can bind through nitrogen and phosphorus {*e.g.* $[Pd(Ph_2PNPh)(PPh_3)]$} and can also bridge two metal centres {*e.g.* $[\{M(Ph_2PNPh)(Ph_2PNHPh)\}_2]$, M = Pd, Pt}. The lithiated ligand was however also found to disproportionate readily in reactions with Ni to give a new bidentate N–P–N ligand $[(NPh)_2PPh_2]$ together with a bridging PPh_2 ligand. In fact, the chemistry of these systems is dominated by the tendency for disproportionation and cleavage of the P–N bond.

Roesky *et al.* prepared $[Li(THF)_4][(Ph_2P–NPh)_4Ln]$ (Ln = Y, Yb and Lu) using the same lithiated ligand ($Ph_2P–NPh^-$ Li^+). These complexes are eight coordinate incorporating four η^2-P–N ligands.[18] Subsequent work by Kühl *et al.* showed that Zr complexes of the same ligand could be prepared with the same coordination geometry.[19,20] They also prepared the Ti complex $[TiCl_2\{N(PPh_2)_2\}_2]$, by reaction of $TiCl_4$ with $Li[N(PPh_2)_2]$, in which the P–N–P ligand binds in the same η^2-fashion with the second phosphorus uncoordinated.

We here report our efforts to prepare the hitherto unknown phosphorus(III) substituted analogues [*e.g.* $R_2P(III)NM$] of the isodiazene ligand systems and to study their chemistry and the nature of the bonding when coordinated. We have adopted the diarylphosphazene nomenclature for these complexes to parallel that for the NNR_2 (isodiazine) analogues, although the calculations and observed chemistry suggest that there is no P–N multiple bonding and that the formal charge is 2−. We also report investigations into the synthesis of complexes of ligands $[R_2P–NR']^-$ and the impact of the nature of R′ on the complex stability.

Experimental

General procedures

All reactions were carried out using standard Schlenk-line techniques under an atmosphere of dry N_2. CH_2Cl_2 and MeCN were both dried by distillation from CaH_2, Et_2O was dried by distillation from Na/benzophenone. All solvents were degassed thoroughly with N_2 before use. All reagents were purchased from Aldrich and used as received unless stated otherwise. $Ph_2PN(SiMe_3)_2$ was prepared according to the literature

DOI: 10.1039/b417068g

procedure,[21,22] but was used without distillation as this caused extensive decomposition. $Ph_2PNHNMe_2$ was prepared according to the literature method.[23,24] $(C_5H_5)TiCl_3$ was prepared from $(C_5H_5)_2TiCl_2$ and $TiCl_4$ by the literature procedure.[25,26]

All ^1H, $^{13}C\{^1H\}$ and $^{31}P\{^1H\}$ NMR spectra were recorded on a Varian Mercury VX 300 spectrometer (^1H at 300 MHz, $^{13}C\{^1H\}$ at 75.5 MHz and $^{31}P\{^1H\}$ at 121.5 MHz) or a Varian Unit 500 MHz spectrometer (^1H at 499.9 MHz, $^{13}C\{^1H\}$ at 125.7 MHz and ^{31}P at 202.4 MHz). Chemical shifts were referenced against the internal solvent. Mass spectra were recorded on a Micromass LCT ToF Spectrometer. IR spectra were recorded on a Perkin-Elmer 1710 spectrometer as KBr disks. Elemental analyses were performed by the microanalysis laboratory of the Inorganic Chemistry Laboratory, University of Oxford.

Preparations

Preparation of $[WCl_4(NPPh_2)]$, 1. $Ph_2PN(SiMe_3)_2$ (0.508 g 1.47 mmol) was dissolved in Et_2O (15 cm^3) to give a pale yellow solution. WCl_6 (0.518 g, 1.47 mmol) was dissolved in Et_2O (15 cm^3) to give and intense orange–brown coloured solution. The $Ph_2PN(SiMe_3)_2$ solution was added to the WCl_6 solution and a colour change to intense dark blue was observed over a few minutes. The solvent was removed under vacuum to leave a sticky dark blue solid which was re-dissolved in CH_2Cl_2 (10 cm^3). The solution was filtered and the volume was then reduced to *ca.* 3 cm^3 and Et_2O (15 cm^3) added to precipitate a sticky dark blue solid. The filtrate was removed and Et_2O (10 cm^3) was added, after stirring for 30 min a fine dark blue powdery solid formed which was collected by filtration, washed with Et_2O (2 × 5 cm^3) and then dried under vacuum (0.360 g, 0.691 mmol, 47% yield). Elemental analysis for $C_{12}H_{10}Cl_4NPW$, found (calc.%): C 27.2 (27.4), H 2.2 (1.9), N 2.3 (2.7). ^1H NMR (CD_2Cl_2): δ 7.2–7.8 (m, 10H, Ph). $^{31}P\{^1H\}$ NMR (CD_2Cl_2): δ 68 (s, $NPPh_2$). IR/cm^{-1} (KBr disk): 3405 (m, br), 2963 (m), 1731 (w), 1636 (w), 1590 (w), 1540 (w), 1439 (s, ν_{P-Ph}), 1292 (s), 1131 (s, ν_{W-N-P}), 1096 (s), 1023 (s), 801 (s), 752 (w), 730 (m), 691 (m), 520 (m).

Preparation of $[WCl_4(NPPh_2)(PMe_2Ph)]$, 2. $Ph_2PN(SiMe_3)_2$ (0.474 g, 1.37 mmol) was dissolved in Et_2O (10 cm^3) to give a pale yellow solution. WCl_6 (0.498 g, 1.26 mmol) was dissolved in Et_2O (10 cm^3) to give an intense dark orange–brown solution. The $Ph_2PN(SiMe_3)_2$ solution was added to the WCl_6 and a colour change to intense dark blue was observed over a few minutes. The solvent was removed under vacuum to leave a sticky dark blue solid which was re-dissolved in CH_2Cl_2 (10 cm^3). A solution of PMe_2Ph (0.18 cm^3, 1.25 mmol) in CH_2Cl_2 (5 cm^3) was added to the reaction mixture and a colour change to intense red–brown was observed. The solution was filtered and then the volume was reduced to *ca.* 5 cm^3, Et_2O (20 cm^3) was added and a dark red–brown solid was formed. The solid was collected by filtration, washed with Et_2O (2 × 5 cm^3) and then dried under vacuum (0.331 g, 0.47 mmol, 37% yield). Elemental analysis for $C_{20}H_{21}Cl_4NP_2W$, found (calc.%): C 36.4 (36.2), H 2.9 (3.2), N 1.6 (2.1). ^1H NMR (CD_2Cl_2): δ 7.2–7.8 (m, 15H, Ph), 5.2 (s, 6H, Me). $^{31}P\{^1H\}$ NMR (CD_2Cl_2): δ 37 (s, $NPPh_2$), 28.6 (s, PMe_2Ph). IR/cm^{-1} (KBr disk): 3385 (s, br), 3060 (m), 2987 (m), 1730 (w), 1654 (w), 1636 (w), 1590 (w), 1541 (w), 1436 (s, ν_{P-Ph}), 1416 (m), 1282 (m), 1125 (s, ν_{W-N-P}), 943 (s), 908 (s), 743 (s), 728 (m), 693 (s), 549 (m), 483 (m).

Preparation of $[WCl_5(NPPh_2)][NBu_4]$, 3. $Ph_2PN(SiMe_3)_2$ (0.448 g, 1.30 mmol) was dissolved in Et_2O (10 cm^3) to give a pale yellow solution. WCl_6 (0.511 g, 1.29 mmol) was dissolved in Et_2O (10 cm^3) to give an intense dark orange–brown solution. The $Ph_2PN(SiMe_3)_2$ solution was added to the WCl_6 solution and a colour change to intense dark blue was observed over a few minutes. The solvent was removed under vacuum to leave a sticky dark blue solid which was re-dissolved in CH_2Cl_2 (10 cm^3). A solution of NBu_4Cl (0.354 g, 1.27 mmol, vacuum dried at 120 °C for 48 h) in CH_2Cl_2 (5 cm^3) was added to the reaction mixture and a colour change to dark grey–purple was observed. The volume was then reduced to *ca.* 2 cm^3 and then Et_2O (10 cm^3) was added to precipitate an oily blue–purple solid. The filtrate was removed and then another portion of Et_2O was added (10 cm^3) and the mixture was left to stir for 30 min forming a fine blue–purple powder which was collected by filtration, washed with Et_2O (5 cm^3) and then dried under vacuum (0.378 g, 0.47 mmol, 36% yield). Elemental analysis for $C_{28}H_{37}Cl_5N_2PW$, found (calc.%): C 41.4 (41.9), H 5.2 (5.8), N 3.2 (3.5). ^1H NMR (CD_2Cl_2): δ 7.4–8.0 (weak m), 3.2 (br s, 2H, $-CH_2(CH_2)_2CH_3$), 1.65 (br s, 2H, $CH_2CH_2CH_2CH_3$), 1.35 (br s, 2H, $(CH_2)_2CH_2CH_3$), 0.9 (br s, 3H, $(CH_2)_3CH_3$). IR/cm^{-1} (KBr disk): 3385 (m, br), 3058 (w), 2960 (s), 2873 (s), 1615 (w), 1590 (w), 1481 (s), 1438 (s, ν_{P-Ph}), 1381 (m), 1264 (m, br), 1127 (s, ν_{W-N-P}), 1090 (m), 1027 (w), 996 (w), 882 (w), 749 (m), 728 (s), 691 (s), 552 (m), 518 (m).

Preparation of $[ReCl_2(MeCN)(PPh_3)_2(N{=}C(CH_3)P(O)Ph_2)]$, 4.

Method A. $[ReOCl_3(PPh_3)_2]$ (0.998 g, 1.20 mmol) was placed in a Schlenk flask and MeCN (10 cm^3) was added to give a lime green suspension. $Ph_2PN(SiMe_3)_2$ (0.469 g, 1.36 mmol) was dissolved in MeCN (10 cm^3) to give a pale yellow solution. The $Ph_2PN(SiMe_3)_2$ solution was added to the $ReOCl_3(PPh_3)_2$ suspension and then the mixture was heated under reflux for 2 h. The dark green–brown solution was filtered hot into a clean flask and then allowed to cool overnight. A green crystalline material (**4**) formed which was collected by filtration and washed with MeCN (2 × 5 cm^3) and then Et_2O (2 × 5 cm^3) and then dried under vacuum (0.147 g, 0.14 mmol, 9% yield).

Method B. $[ReOCl_3(PPh_3)_2]$ (0.998 g, 1.20 mmol) was placed in a Schlenk flask along with $Ph_2PN(SiMe_3)_2$ (0.413 g, 1.20 mmol) and PPh_3 (0.692 g 2.64 mmol). MeCN (15 cm^3) was added to give a lime green suspension and the mixture was then heated under reflux for 2 h. The solution was filtered hot to collect a green crystalline material, **4**, which was washed with MeCN (2 × 5 cm^3) and dried under vacuum (0.432 g, 0.41 mmol, 34% yield). The filtrate was left to cool and after 24 h a mixture of green and orange crystals had formed in the solution (0.169 g). The green crystals were identified as the desired product (**4**) and the orange crystals as $[Re(MeCN)Cl_3(PPh_3)_2]$. Analysis of **4**: ^1H NMR (CD_2Cl_2): δ 6.80–7.70 (m, 40H, $P(C_6H_5)_3$ and $-P(O)(C_6H_5)_2$), 2.85 (d, $^3J_{H-P} = 9$ Hz, 3H, $N{=}C(CH_3)P$), 2.20 (s, 3H, MeCN). $^{31}P\{^1H\}$ NMR (CD_2Cl_2): δ 6 (s, $P(O)Ph_2$), −11 (s, PPh_3). MS (ES): *m/z* 1024 [M − MeCN]. IR/cm^{-1} (KBr disk): 3414 (m, br), 3053 (m), 2918 (w), 1541 (m, $\nu_{C=N}$), 1483 (m), 1434 (s), 1358 (w), 1189 (m), 1114 (m), 1093 (m), 999 (m), 771 (w), 748 (m), 721 (m), 696 (s), 585 (m), 560 (m), 541 (m), 519 (s), 500 (m).

Preparation of $[ReBr_2(MeCN)(PPh_3)_2(N{=}C(CH_3)P(O)Ph_2)]$, 5. $[ReOBr_3(PPh_3)_2]$ (0.501 g, 0.52 mmol) was placed in a Schlenk flask along with $Ph_2PN(SiMe_3)_2$ (0.184 g, 0.53 mmol) and PPh_3 (0.301 g, 1.15 mmol). MeCN (15 cm^3) was added to give a dark yellow suspension and the mixture was then heated under reflux for 2 h. The solution was filtered hot to collect a green crystalline material, **5**, which was washed with MeCN (2 × 5 cm^3) and then dried under vacuum (0.311 g, 0.27 mmol, 52% yield). The filtrate was left to cool and after 24 h a mixture of green and orange/brown crystals formed from the solution (0.106 g). The green crystals were identified as the product described previously (**5**), and the orange–brown crystals as $[Re(MeCN)Br_3(PPh_3)_2]$. Analysis of **5**: ^1H NMR ($CDCl_3$): δ 6.86–7.85 (m, 40H, $P(C_6H_5)_3$ and $-P(O)(C_6H_5)_2$), 3.10 (d, $^3J_{H=P} = 10$ Hz, 3H, $N{=}C(CH_3)P$), 2.28 (s, 3H, MeCN). $^{31}P\{^1H\}$ NMR (CD_2Cl_2): δ 4 (s, $N{=}C(CH_3)P(O)Ph_2$), −17 (s, PPh_3). MS (FAB$^+$): *m/z* 1033 $[M - Br]^+$, 1074 $[M - MeCN - Br)]^+$. IR/cm^{-1} (KBr disk): 3052 (w), 1542 (m, $\nu_{C=N}$), 1482 (m), 1434 (s), 1400 (m), 1361 (w), 1184 (w), 1114 (w), 1092 (m), 998 (w), 770 (w), 746 (m), 721 (w), 695 (s), 583 (w), 558 (w), 540 (w), 520 (s).

Analysis of $[Re(MeCN)Br_3(PPh_3)_2]$. MS (FAB$^+$): *m/z* 991 $[M]^+$, 950 $[M - MeCN]^+$, 871 $[M - Br - MeCN)]^+$. IR/cm^{-1} (KBr disk): 3433 (br, w), 3056 (w), 1482 (m), 1434 (s), 1187 (w),

1090 (s), 1025 (w), 998 (w), 745 (s), 696 (s), 517 (s), 497 (m), 458 (w).

Preparation of 2-diphenylphosphino-1,1-dimethylhydrazine (L^2H). $Ph_2PNHNMe_2$ was prepared according to the literature,[23,24] producing a free flowing white solid (3.95 g, 16.2 mmol, 90% yield). ^1H NMR (CD_2Cl_2): δ 7.5–7.6 (m, 4H, *o*-Ph), 7.3–7.5 (m, 6H, *m*- and *p*-Ph), 3.31 (d, $^2J_{H-P} = 12$ Hz, 1H, NH), 2.46 (s, 6H, $N(CH_3)_2$). $^{13}C\{^1H\}$ NMR (CD_2Cl_2): δ 132.2 (d, $^2J_{C-P} = 20$ Hz, *o*-C), 129.0 (s, *p*-C), 128.4 (d, $^3J_{C-P} = 5.2$ Hz, *m*-C), 51.1 (s, CH_3). $^{31}P\{^1H\}$ NMR (CD_2Cl_2): δ 38.6 (s). MS (ES^+): *m*/*z* 245 $[L + H]^+$.

Preparation of 1-diphenylphosphinoamino-4-methylpiperazine (L^3H). To a clear colourless solution of 1-amino-4-methylpiperazine (1.72 g, 1.8 cm^3, 15 mmol) and triethylamine (1.5 g, 2.1 cm^3, 15 mmol) in Et_2O (15 cm^3), chlorodiphenylphosphine (3.3 g, 2.7 cm^3, 15 mmol) was added dropwise over 10 min whilst cooling in an ice bath, producing a white precipitate immediately. The mixture was slowly warmed to room temperature and stirred for a further 1 h. The solid produced was removed by filtration and washed with Et_2O (2 × 15 cm^3). The Et_2O solutions were combined, evaporated to dryness and dried under vacuum producing a clear, colourless oil in quantitative yield. Elemental analysis for $C_{17}H_{22}N_3P$, found (calc.%): C 68.2 (68.2), H 7.9 (7.4), N 13.7 (14.0). ^1H NMR ($CDCl_3$): δ 7.45–7.6 (m, 4H, *o*-Ph), 7.3–7.45 (m, 6H, *m*- and *p*-Ph), 3.35 (d, $^2J_{H-P} = 10$ Hz, 1H, NH), 2.3–3.0 (m, br, 8H, $N(C_2H_4)_2NCH_3$), 2.27 (s, 3H, NCH_3). $^{13}C\{^1H\}$ NMR ($CDCl_3$): δ 131.9 (d, $^2J_{C-P} = 20$ Hz, *o*-Ph), 128.7 (s, *p*-Ph), 128.2 (d, $^3J_{C-P} = 7$ Hz, *m*-Ph), 59.1 (d, $^3J_{C-P} = 4$ Hz, $NHNCH_2$), 55.0 (s, CH_2NCH_3), 45.7 (s, NCH_3). $^{31}P\{^1H\}$ NMR ($CDCl_3$): δ 39.2 (s). Selected IR/cm^{-1} (pure oil): 3196 (w, br, ν_{N-H}), 3052 (m, $\nu_{C-Haromatic}$), 1585 (w, ν_{N-H}), 1434 (s, ν_{P-Ph}), 954 (w, ν_{N-N}), 743 (s, ν_{P-N}).

Preparation of 1-diphenylphosphinoaminopiperidine (L^4H). To a clear colourless solution of 1-aminopiperidine (1.4 g, 1.5 cm^3, 14 mmol) and triethylamine (1.5 g, 2.1 cm^3, 15 mmol) in Et_2O (15 cm^3), chlorodiphenylphosphine (3.1 g, 2.5 cm^3, 14 mmol) was added dropwise over 10 min at −78 °C, producing a white precipitate immediately. The mixture was then warmed to room temperature over the period of 30 min and stirred for a further 1 h. The solid produced was removed by filtration and washed with Et_2O (3 × 10 cm^3). The Et_2O solutions were combined, evaporated to dryness and dried under vacuum at 80 °C producing a clear colourless oil in quantitative yield. Elemental analysis for $C_{17}H_{21}N_2P$, found (calc.%): C 72.0 (71.8), H 7.4 (7.4), N 9.5 (9.8). ^1H NMR ($CDCl_3$): δ 7.35–7.45 (m, 4H, *o*-Ph), 7.2–7.3 (m, 6H, *m*- and *p*-Ph), 3.25 (d, $^2J_{H-P} = 8$ Hz, 1H, NH), 2.52 (m, 4H, $N(CH_2CH_2)_2CH_2$), 1.49 (m, 4H, $N(CH_2CH_2)_2CH_2$), 1.23 (m, 2H, $N(CH_2CH_2)_2CH_2$). $^{13}C\{^1H\}$ NMR ($CDCl_3$): δ 131.8 (d, $^2J_{C-P} = 20$ Hz, *o*-Ph), 128.6 (s, *p*-Ph), 128.1 (d, $^3J_{C-P} = 6$ Hz, *m*-Ph), 60.9 (d, $^3J_{C-P} = 4$ Hz, $N(CH_2CH_2)_2CH_2$), 26.0 (s, $N(CH_2CH_2)_2CH_2$), 23.4 (s, $N(CH_2CH_2)_2CH_2$). $^{31}P\{^1H\}$ NMR ($CDCl_3$): δ 35.6 (s). Selected IR/cm^{-1} (pure oil): 3224 (w, br, ν_{N-H}), 3052 (m, $\nu_{C-Haromatic}$), 1586 (w, ν_{N-H}), 1434 (s, ν_{P-Ph}), 966 (w, ν_{N-N}), 742 (s, ν_{P-N}).

Preparation of $[(C_5H_5)TiCl_2(Ph_2PNNMe_2)]$, 6. To a clear colourless solution of L^2H (0.5 g, 2.05 mmol) in Et_2O (15 cm^3), $[(C_5H_5)TiCl_3]$ (0.225 g, 1.03 mmol) was added, producing a bright yellow solution and white precipitate immediately. The mixture was stirred at room temperature for 2 h and then cooled to −78 °C and stirred for a further 2 h. The white precipitate was then removed by filtration at −18 °C, and the bright yellow Et_2O solution left to stand, producing large bright orange crystals suitable for X-ray analysis. The remaining Et_2O solution was evaporated to dryness producing a bright yellow–orange crystalline solid (0.35 g, 0.82 mmol, 80% yield). Elemental analysis for $C_{19}H_{21}Cl_2N_2PTi$, found (calc.%): C 53.7 (53.4), H 5.3 (5.0), N 6.4 (6.6), Cl 16.4 (16.6). ^1H NMR ($CDCl_3$): δ 7.4–7.5 (m, 6H, *m*- and *p*-Ph), 7.3–7.4 (m, 4H, *o*-Ph), 6.19 (s, 5H, C_5H_5), 3.10 (s, 6H, $N(CH_3)_2$). $^{13}C\{^1H\}$ NMR ($CDCl_3$): δ 131.7 (d, $^2J_{C-P} = 20$ Hz, *o*-Ph), 129.7 (s, *p*-Ph), 128.9 (d, $^3J_{C-P} = 6$ Hz, *m*-Ph), 118.1 (s, C_5H_5), 50.4 (d, $^3J_{C-P} = 10$ Hz, NCH_3). $^{31}P\{^1H\}$ NMR ($CDCl_3$): δ 55.8 (s). Selected IR/cm^{-1} (KBr disk): 2961 (s, br, ν_{C-H}), 1434 (s, ν_{P-Ph}), 742 (s, ν_{P-N}).

Preparation of $[RuCl_2(\eta^6\text{-}p\text{-}MeC_6H_4{}^iPr)(L^2H)]$, 7. To a clear colourless solution of L^2H (0.5 g, 2.05 mmol) in THF (15 cm^3), $[\{RuCl(\mu\text{-}Cl)(\eta^6\text{-}p\text{-}MeC_6H_4{}^iPr)\}_2]$ (0.612 g, 1.0 mmol) was added, producing a dark red suspension. The mixture was heated under reflux for 1 h and then allowed to cool to room temperature. The volume was reduced by half and the solution cooled to 0 °C producing a red precipitate which was isolated by filtration and washed with cold THF (5 cm^3) and pentane (2 × 5 cm^3). It was then recrystallized from CH_2Cl_2–pentane, and dried under vacuum (0.85 g, 1.5 mmol, 77% yield). Elemental analysis for $C_{24}H_{31}Cl_2N_2PRu$, found (calc.%): C 52.8 (52.4), H 5.7 (5.7), N 4.8 (5.1), Cl 12.8 (12.9). ^1H NMR ($CDCl_3$): δ 7.92 (m, 4H, *o*-Ph), 7.3–7.5 (m, 6H, *m*- and *p*-Ph), 5.19 (d, $^3J_{H-H} = 5$ Hz, 2H, $CHC(Me)$), 5.01 (d, $^3J_{H-H} = 5$ Hz, 2H, $CHC(^iPr)$), 3.95 (d, $^2J_{H-P} = 30$ Hz, 1H, NH), 2.46 (septet, $^3J_{H-H} = 7$ Hz, 1H, $RCHMe_2$), 1.95 (s, 6H, $N(CH_3)_2$), 1.86 (s, 3H, $CHC(CH_3)$), 0.78 (d, $^3J_{H-H} = 7$ Hz, 6H, $RCH(CH_3)_2$). $^{13}C\{^1H\}$ NMR ($CDCl_3$): δ 134.4 (d, $^1J_{C-P} = 45$ Hz, *i*-Ph), 133.8 (d, $^2J_{C-P} = 11$ Hz, *o*-Ph), 130.7 (d, $^4J_{C-P} = 2$ Hz, *p*-Ph), 127.7 (d, $^3J_{C-P} = 10$ Hz, *m*-Ph), 108.0 (s, $C(^iPr)$), 94.8 (s, $C(Me)$), 90.6 (d, $^2J_{C-P} = 5$ Hz, $CHCMe$), 86.5 (d, $^2J_{C-P} = 6$ Hz, $CHC(^iPr)$), 49.5 (s, NCH_3), 30.0 (s, $RCHMe_2$), 21.5 (s, $RCH(CH_3)_2$), 17.4 (s, $CHC(CH_3)$). $^{31}P\{^1H\}$ NMR ($CDCl_3$): δ 65.7 (s). MS (ES^+): *m*/*z* 551.5 $[M + H]^+$. Selected IR/cm^{-1} (KBr disk): 3275 (m, sh, ν_{N-H}), 1435 (s, ν_{P-Ph}), 747 (s, ν_{P-N}).

Preparation of $[RuCl_2(\eta^6\text{-}p\text{-}MeC_6H_4{}^iPr)(L^3H)]$, 8. To a clear colourless solution of L^3H (0.40 g, 1.3 mmol) in THF (15 cm^3), $[\{RuCl(\mu\text{-}Cl)(\eta^6\text{-}p\text{-}MeC_6H_4{}^iPr)\}_2]$ (0.413 g, 0.65 mmol) was added, producing a dark orange–brown suspension. The mixture was stirred at room temperature for 18 h, during which time a precipitate formed. The solid was isolated by filtration, washed with THF (2 × 5 cm^3) and dried under vacuum, yielding a red–brown microcrystalline solid (0.67 g, 1.1 mmol, 85% yield). Elemental analysis for $C_{27}H_{36}Cl_2N_3PRu$, found (calc.%): C 53.7 (53.6), H 6.0 (6.0), N 6.9 (6.9). ^1H NMR ($CDCl_3$): δ 7.85–8.0 (m, 4H, *o*-Ph), 7.35–7.45 (m, 6H, *m*- and *p*-Ph), 5.22 (d, $^3J_{H-H} = 6$ Hz, 2H, $CHC(Me)$), 5.03 (d, $^3J_{H-H} = 6$ Hz, 2H, $CHC(^iPr)$), 4.10 (d, $^2J_{H-P} = 30$ Hz, 1H, NH), 2.44 (septet, $^3J_{H-H} = 7$ Hz, 1H, $RCHMe_2$), 2.22 (m, 4H, $N(CH_2CH_2)_2NCH_3$), 1.99 (m, 7H, $N(CH_2CH_2)_2NCH_3$ and $N(CH_2CH_2)_2NCH_3$), 1.86 (s, 3H, $CHC(CH_3)$), 0.78 (d, $^3J_{H-H} = 7$ Hz, 6H, $RCH(CH_3)_2$). $^{13}C\{^1H\}$ NMR ($CDCl_3$): δ 134.6 (d, $^1J_{C-P} = 56$ Hz, *i*-Ph), 133.9 (d, $^2J_{C-P} = 11$ Hz, *o*-Ph), 130.7 (d, $^4J_{C-P} = 2$ Hz, *p*-Ph), 127.6 (d, $^3J_{C-P} = 10$ Hz, *m*-Ph), 108.0 (s, $C(^iPr)$), 94.8 (s, $C(Me)$), 90.5 (d, $^2J_{C-P} = 5$ Hz, $CHC(Me)$), 86.6 (d, $^2J_{C-P} = 6$ Hz, $CHC(^iPr)$), 57.1 (d, $^3J_{C-P} = 3$ Hz, $N(CH_2CH_2)_2NCH_3$), 54.8 and 45.6 (s, $N(CH_2CH_2)_2NCH_3$ and $N(CH_2CH_2)_2NCH_3$), 29.9 (s, $RCHMe_2$), 21.4 (s, $RCH(CH_3)_2$), 17.4 (s, $CHC(CH_3)$). $^{31}P\{^1H\}$ NMR ($CDCl_3$): δ 67.9 (s). MS (ES^+): *m*/*z* 605.6 $[M + H]^+$. Selected IR/cm^{-1} (KBr disk): 3236 (m, sh, ν_{N-H}), 1437 (s, ν_{P-Ph}), 743 (s, ν_{P-N}).

Preparation of $[RuCl_2(\eta^6\text{-}p\text{-}MeC_6H_4{}^iPr)(L^4H)]$, 9. To a clear colourless solution of L^4H (0.5 g, 1.75 mmol) in THF (20 cm^3), $[\{RuCl(\mu\text{-}Cl)(\eta^6\text{-}p\text{-}MeC_6H_4{}^iPr)\}_2]$ (0.538 g, 0.88 mmol) was added, producing a dark orange–brown suspension. The mixture was stirred at room temperature for 2 h, during which time a precipitate formed. The volume of the solution was reduced to *ca.* 5 cm^3, and pentane (30 cm^3) was added to complete precipitation. The solid was isolated by filtration, washed with pentane (2 × 5 cm^3) and dried under vacuum, producing an orange–red solid (0.97 g, 1.6 mmol, 91% yield). Elemental analysis for $C_{27}H_{35}Cl_2N_2PRu{\cdot}CH_2Cl_2$, found (calc.%): C 50.0 (49.8), H 5.8 (5.5), N 4.2 (4.2). ^1H NMR ($CDCl_3$): δ 7.91

(m, 4H, *o*-Ph), 7.35–7.45 (m, 6H, *m*- and *p*-Ph), 5.20 (d, $^3J_{H-H}$ = 6 Hz, 2H, C*H*C(Me)), 5.00 (d, $^3J_{H-H}$ = 6 Hz, 2H, C*H*C(^{i}Pr)), 4.00 (d, $^2J_{H-P}$ = 31 Hz, 1H, NH), 2.43 (septet, $^3J_{H-H}$ = 7 Hz, 1H, RC*H*Me$_2$), 2.13 (m, 4H, N(C*H*$_2$CH$_2$)$_2$CH$_2$), 1.86 (s, 3H, CHC(C*H*$_3$)), 1.06 (m, 6H, N(CH$_2$C*H*$_2$)$_2$CH$_2$ and N(CH$_2$CH$_2$)$_2$C*H*$_2$), 0.79 (d, $^3J_{H-H}$ = 7 Hz, 6H, RCH(C*H*$_3$)$_2$). ^{13}C{^{1}H} NMR (CDCl$_3$): δ 134.8 (d, $^1J_{C-P}$ = 56 Hz, *i*-Ph), 134.0 (d, $^2J_{C-P}$ = 10 Hz, *o*-Ph), 130.6 (d, $^4J_{C-P}$ = 2 Hz, *p*-Ph), 127.5 (d, $^3J_{C-P}$ = 10 Hz, *m*-Ph), 107.9 (s, *C*(^{i}Pr)), 94.8 (s, *C*(Me)), 90.4 (d, $^2J_{C-P}$ = 5 Hz, *C*HC(Me)), 86.5 (d, $^2J_{C-P}$ = 6 Hz, *C*HC(^{i}Pr)), 58.9 (d, $^3J_{C-P}$ = 3 Hz, N(*C*H$_2$CH$_2$)$_2$CH$_2$), 29.9 (s, R*C*HMe$_2$), 25.9 (s, N(CH$_2$*C*H$_2$)$_2$CH$_2$), 23.3 (s, N(CH$_2$CH$_2$)$_2$*C*H$_2$), 21.5 (s, RCH(*C*H$_3$)$_2$), 17.4 (s, CHC(*C*H$_3$)). ^{31}P{^{1}H} NMR (CDCl$_3$): δ 66.4 (s). MS (ES$^+$): *m*/*z* 591 [M + H]$^+$, 555 [M − Cl]$^+$. Selected IR/cm^{-1} (KBr disk): 3299 (m, sh, ν_{N-H}), 1433 (s, ν_{P-Ph}), 746 (s, ν_{P-N}).

Preparation of [RuCl(η^6-*p*-MeC$_6$H$_4$^{i}Pr)(L^{2}H)]$^+$[BF$_4$]$^-$, 10. To a dark red–brown solution of **7** (0.25 g, 0.45 mmol) in toluene (15 cm^3), AgBF$_4$ (0.092 g, 0.47 mmol) was added in the dark, producing an orange precipitate almost immediately. The mixture was stirred at room temperature for 30 min and the solid was then isolated by filtration in the dark. The orange solid was dissolved in CH$_2$Cl$_2$ (10 cm^3) and the solution filtered through Celite, the volume reduced to *ca.* 3 cm^3 and Et$_2$O (20 cm^3) added to precipitate a microcrystalline yellow–orange solid (0.24 g, 0.40 mmol, 89% yield). Elemental analysis for C$_{24}$H$_{31}$BClF$_4$N$_2$PRu, found (calc.%): C 47.5 (47.9), H 5.6 (5.2), N 4.8 (4.7). ^{1}H NMR (CD$_2$Cl$_2$): δ 7.5–7.8 (m, 10H, Ph), 7.31 (d, $^2J_{H-P}$ = 3 Hz, 1H, NH), 6.06 (d, $^3J_{H-H}$ = 6 Hz, 1H, C*H*C(^{i}Pr)), 5.70 (d, $^3J_{H-H}$ = 6 Hz, 1H, C*H*C(Me)), 5.50 (d, $^3J_{H-H}$ = 6 Hz, 1H, C*H*C(Me)), 5.42 (d, $^3J_{H-H}$ = 6 Hz, 1H, C*H*C(^{i}Pr)), 3.60 and 2.86 (s, 6H, N(C*H*$_3$)$_2$), 2.82 (septet, $^3J_{H-H}$ = 7 Hz, 1H, RC*H*Me$_2$), 1.62 (s, 3H, CHC(C*H*$_3$)), 1.31 (d, $^3J_{H-H}$ = 7 Hz, 3H RCHC*H*$_3$), 1.27 (d, $^3J_{H-H}$ = 7 Hz, 3H RCHC*H*$_3$). ^{13}C{^{1}H} NMR (CD$_2$Cl$_2$): δ 129–132 (m, Ph), 119.1 (s, *C*(^{i}Pr), 99.2 (s, CH*C*(Me)), 88.4 (s, *C*HC(Me)), 86.8 (s, *C*HC(^{i}Pr)), 84.1 (s, *C*HC(^{i}Pr)), 83.0 (s, *C*HC(Me)), 64.7 and 55.8 (s, N(*C*H$_3$)$_2$), 31.4 (s, R*C*HMe$_2$), 22.7 and 21.3 (s, RCH(*C*H$_3$)$_2$), 17.3 (s, C(*C*H$_3$)). ^{31}P{^{1}H} NMR (CD$_2$Cl$_2$): δ 43.7 (s). MS (ES$^+$): *m*/*z* 515.02 [M]$^+$. Selected IR/cm^{-1} (KBr disk): 3279 (m, sh, ν_{N-H}), 1437 (s, sh, ν_{P-Ph}), 748 (m, sh, ν_{P-N}).

Preparation of [RuCl(η^6-*p*-MeC$_6$H$_4$^{i}Pr)(LL^{3}H)]$^+$[BF$_4$]$^-$, 11. To a dark red–brown solution of **8** (0.27 g, 0.45 mmol) in toluene (15 cm^3), a benzene solution (15 cm^3) of AgBF$_4$ (0.092 g, 0.47 mmol) was added in the dark over the period of 5 min, producing an orange precipitate immediately. The mixture was stirred at room temperature for 30 min and then left to stand for a further 1 h. The solid was isolated by filtration, washed with warm toluene (2 × 15 cm^3), dissolved in CH$_2$Cl$_2$ (10 cm^3) and left to stand for a further 5 min. This suspension was filtered through Celite and the volume reduced under vacuum to *ca.* 2 cm^3. Pentane was added to precipitate the product as an ochre coloured solid, which was isolated by filtration and dried under vacuum (0.27 g, 0.41 mmol, 93% yield). Elemental analysis for C$_{27}$H$_{36}$BClF$_4$N$_3$PRu, found (calc.%): C 49.1 (49.4), H 5.6 (5.5), N 6.2 (6.4), Cl 5.0 (5.4). ^{1}H NMR (CD$_2$Cl$_2$): δ 7.3–7.6 (m, 10H, Ph), 7.09 (d, $^2J_{H-P}$ = 3 Hz, 1H, NH), 5.96 (d, $^3J_{H-H}$ = 6 Hz, 1H, η^6-*p*-MeC$_6$*H*$_4$^{i}Pr), 5.45 (d, $^3J_{H-H}$ = 7 Hz, 1H, η^6-*p*-MeC$_6$*H*$_4$^{i}Pr), 5.37 (d, $^3J_{H-H}$ = 6 Hz, 1H, η^6-*p*-MeC$_6$*H*$_4$^{i}Pr), 5.07 (d, $^3J_{H-H}$ = 7 Hz, 1H, η^6-*p*-MeC$_6$*H*$_4$^{i}Pr), 3.65 (m, 1H, N(C$_2$*H*$_4$)$_2$NCH$_3$), 3.17 (m, 1H, N(C$_2$*H*$_4$)$_2$NCH$_3$), 2.85 (m, 1H, N(C$_2$*H*$_4$)$_2$NCH$_3$), 2.76 (septet, $^3J_{H-H}$ = 7 Hz, 1H, RC*H*Me$_2$), 2.2–2.6 (m, 5H, N(C$_2$*H*$_4$)$_2$NCH$_3$), 2.25 (s, 3H, NCH$_3$), 1.42 (s, 3H, CHC(C*H*$_3$)), 1.22 (d, $^3J_{H-H}$ = 7 Hz, 3H, RCHC*H*$_3$), 1.18 (d, $^3J_{H-H}$ = 7 Hz, 3H, RCHC*H*$_3$). ^{31}P{^{1}H} NMR (CD$_2$Cl$_2$): δ 46.9 (s). MS (ES$^+$): *m*/*z* 570 [M]$^+$. Selected IR/cm^{-1} (KBr disk): 3303 (m, br, ν_{N-H}), 1437 (s, sh, ν_{P-Ph}), 751 (m, sh, ν_{P-N}).

Preparation of [RuCl(η^6-*p*-MeC$_6$H$_4$^{i}Pr)(L^{4}H)]$^+$[BF$_4$]$^-$, 12. To a dark red–brown solution of **9** (0.20 g, 0.34 mmol) in toluene (15 cm^3), a benzene solution (15 cm^3) of AgBF$_4$ (0.058 g, 0.30 mmol) was added in the dark over the period of 5 min, producing an orange precipitate immediately. The mixture was stirred at room temperature for 15 min and then left to stand for *ca.* 1 h. The solid was isolated by filtration, washed with toluene (2 × 10 cm^3), dissolved in CH$_2$Cl$_2$ (15 cm^3) and left to stand for a further 10 min. This suspension was then filtered through Celite and the volume reduced under vacuum to *ca.* 2 cm^3. Pentane was added to precipitate the product as a bright orange microcrystalline solid, which was isolated by filtration and dried under vacuum, (0.155 g, 0.24 mmol, 80% yield). Elemental analysis for C$_{27}$H$_{35}$BClF$_4$N$_2$PRu, found (calc.%): C 50.6 (50.5), H 5.5 (5.5), N 4.3 (4.4). ^{1}H NMR (CD$_2$Cl$_2$): δ 7.5–7.65 (m, 2H, *m*-Ph), 7.4–7.5 (m, 5H, *o*-, *m*- and *p*-Ph), 7.25–7.4 (m, 3H, *o*- and *p*-Ph), 7.01 (d, $^2J_{H-P}$ = 3 Hz, 1H, NH), 6.01 (d, $^3J_{H-H}$ = 6 Hz, 1H, C*H*C(^{i}Pr)), 5.53 (pseudo-quartet, $^3J_{H-H}$ = 6 Hz and $^3J_{H-P}$ = 3 Hz, 1H, C*H*C(Me)), 5.32 (d, $^3J_{H-H}$ = 6 Hz, 1H, C*H*C(Me)), 4.96 (d, $^3J_{H-H}$ = 6 Hz, 1H, C*H*C(^{i}Pr)), 3.4–3.6 (m, 2H, N(C*H*$_2$CH$_2$)$_2$CH$_2$), 3.1–3.2 (m, 1H, N(C*H*$_2$CH$_2$)$_2$CH$_2$), 2.76 (m, 1H, N(C*H*$_2$CH$_2$)$_2$CH$_2$), 2.70 (septet, $^3J_{H-H}$ = 7 Hz, 1H, RC*H*Me$_2$), 1.9–2.1 (m, 1H, N(CH$_2$C*H*$_2$)$_2$CH$_2$), 1.4–1.6 (m, 3H, N(CH$_2$C*H*$_2$)$_2$CH$_2$), 1.34 (s, 3H, CHC(C*H*$_3$)), 1.2–1.3 (m, 2H, N(CH$_2$CH$_2$)$_2$C*H*$_2$), 1.20 (d, $^3J_{H-H}$ = 7 Hz, 3H, RCHC*H*$_3$), 1.14 (d, $^3J_{H-H}$ = 7 Hz, 3H, RCHC*H*$_3$). ^{13}C{^{1}H} NMR (CD$_2$Cl$_2$): δ 132.9 (d, $^1J_{C-P}$ = 54 Hz, *i*-Ph), 132.1 (d, $^4J_{C-P}$ = 2 Hz, *p*-Ph), 131.8 (d, $^2J_{C-P}$ = 12 Hz, *o*-Ph), 131.5 (d, $^4J_{C-P}$ = 2 Hz, *p*-Ph), 130.8 (d, $^3J_{C-P}$ = 12 Hz, *m*-PH), 129.8 (d, $^3J_{C-P}$ = 11 Hz, *m*-Ph), 128.5 (d, $^2J_{C-P}$ = 12 Hz, *o*-Ph), 121.0 (d, $^2J_{C-P}$ = 6 Hz, *C*(^{i}Pr)), 99.4 (s, *C*(Me)), 88.2 (s, *C*HC(Me)), 85.9 (d, $^2J_{C-P}$ = 9 Hz, *C*HC(^{i}Pr)), 83.5 (s, *C*HC(Me)), 80.0 (s, *C*HC(^{i}Pr)), 71.8 (d, $^3J_{C-P}$ = 2 Hz, N(*C*H$_2$CH$_2$)$_2$CH$_2$), 62.2 (d, $^3J_{C-P}$ = 5 Hz, N(*C*H$_2$CH$_2$)$_2$CH$_2$), 31.0 (s, R*C*HMe$_2$), 24.1, 23.1 and 22.6 (s, N(CH$_2$*C*H$_2$)$_2$CH$_2$ and N(CH$_2$CH$_2$)$_2$*C*H$_2$), 22.7 (s, RCH(*C*H$_3$)$_2$), 20.7 (s, RCH(*C*H$_3$)$_2$), 16.9 (s, C(*C*H$_3$)). ^{31}P{^{1}H} NMR (CD$_2$Cl$_2$): δ 45.9. MS (ES$^+$): *m*/*z* 555 [M]$^+$. Selected IR/cm^{-1} (KBr disk): 3300 (m, sh, ν_{N-H}), 1436 (s, ν_{P-Ph}), 745 (s, ν_{P-N}).

Preparation of [(η^6-*p*-MeC$_6$H$_4$^{i}Pr)Cl$_2$Ru(μ^2,η^3-PPh$_2$NNMe$_2$)Ti(C$_5$H$_5$)Cl$_2$], 13. To a bright yellow–orange solution of **6** (0.20 g, 0.47 mmol) in THF (10 cm^3), [{RuCl(μ-Cl)(η^6-*p*-MeC$_6$H$_4$^{i}Pr)}$_2$] (0.14 g, 0.228 mmol) was added and the mixture stirred at room temperature for 90 min during which time the solution became dark orange–brown. The volume was then reduced to *ca.* 3 cm^3 and Et$_2$O (45 cm^3) added to cause precipitation. The dark orange solid produced was isolated by filtration, washed with Et$_2$O (2 × 5 cm^3) and dried under vacuum (0.20 g, 0.27 mmol, 61% yield). Elemental analysis for C$_{29}$H$_{35}$Cl$_4$N$_2$PRuTi, found (calc.%): C 47.4 (47.5), H 4.9 (4.8), N 3.8 (3.8), Cl 19.3 (19.3). ^{1}H NMR (CD$_2$Cl$_2$): δ 8.19 (m, 4H, *o*-Ph), 7.48 (m, 6H, *m*- and *p*-Ph), 6.51 (s, 5H, C$_5$H$_5$), 5.06 (d, $^3J_{H-H}$ = 6 Hz, 2H, C*H*C(^{i}Pr)), 4.72 (d, $^3J_{H-H}$ = 6 Hz, 2H, C*H*C(Me)), 2.81 (s, 6H, N(C*H*$_3$)$_2$), 2.51 (septet, $^3J_{H-H}$ = 7 Hz, 1H, RC*H*Me$_2$), 1.63 (s, 3H, CHC(C*H*$_3$)) 1.12 (d, $^3J_{H-H}$ = 7 Hz, 6H, RCH(C*H*$_3$)$_2$). ^{13}C{^{1}H} NMR (CD$_2$Cl$_2$): δ 134.3 (d, $^2J_{C-P}$ = 12 Hz, *o*-Ph), 131.5 (d, $^4J_{C-P}$ = 2 Hz, *p*-Ph), 128.1 (d, $^3J_{C-P}$ = 10 Hz, *m*-Ph), 120.7 (s, C$_5$H$_5$), 112.1 (s, *C*(^{i}Pr)), 98.1 (s, *C*(Me)), 89.0 (d, $^2J_{C-P}$ = 4 Hz, *C*HC(Me)), 88.0 (d, $^2J_{C-P}$ = 6 Hz, *C*HC(^{i}Pr)), 54.1 (s, N*C*H$_3$), 30.2 (s, R*C*HMe$_2$), 22.0 (s, RCH(*C*H$_3$)$_2$), 17.5 (s, CHC(*C*H$_3$)). ^{31}P{^{1}H} NMR (CD$_2$Cl$_2$): δ 86.3 (s). Selected IR/cm^{-1} (KBr disk): 3051 (m, $\nu_{C-Haromatic}$), 2962 (m, $\nu_{C-Haliphatic}$), 1436 (s, ν_{P-Ph}), 739 (s, ν_{P-N}).

Molecular modelling

All calculations were carried out using the Gaussian 98W suite of programs.[27] Becke's three parameter hybrid functional using the correlation functional of Lee, Yang and Parr (B3LYP)[28] was used in conjunction with the standard 6-31g(d)[29–34] basis set for all non-metal atoms, and the LanL2DZ[35–37] basis set

for W of complex **3** and 6-311(g)d[38–42] for complex **6**. The structures were optimised and the presence of a minimum on the potential energy surface was confirmed by a vibrational frequency calculation. The basis sets were chosen in order to provide a trade off between accuracy and computational power required.

Crystallography

X-Ray crystal structures were determined by mounting a single crystal encased in perfluoropolyether oil on a glass fibre and then cooling rapidly to 150 K in a stream of cold N_2 using an Oxford Cryosystems CRYOSTREAM unit. Diffraction data were measured using an Enraf-Nonius KappaCCD diffractometer (graphite-monochromated Mo-Kα radiation, $\lambda =$ 0.71073 Å). Intensity data were processed using the DENZO-SMN package.[43] The structures were solved using the direct-methods program SIR92,[44] which located all non-hydrogen atoms of the complexes. Subsequent full-matrix least-squares refinement was carried out using the CRYSTALS program suite.[45] Hydrogen atoms were positioned geometrically after each cycle of refinement. A three-term Chebychev polynomial weighting scheme was applied. Details of the crystal data and refinement can be found in Tables 1 and 2.

CCDC reference numbers 255284–255294.

See http://www.rsc.org/suppdata/dt/b4/b417068g/ for crystallographic data in CIF or other electronic format.

Results and discussion

Tungsten phosphazene complexes

WCl_6 reacted rapidly with $Ph_2PN(SiMe_3)_2$ in Et_2O to give a dark blue species that analysed as $WCl_4(NPPh_2)$ **1**, the reaction proceeding with the elimination of two molecules of $ClSiMe_3$. Complex **1** showed a single peak at 68 ppm in the $^{31}P\{^1H\}$ NMR spectrum, which is consistent with the P(III)-containing structure proposed. (*cf.* the free ligand at 50.2 ppm).[46] It seems probable that the complex exists as a Cl-bridged dimer to achieve octahedral coordination of the tungsten centres (Fig. 1(A)), as in the analogous isodiazene species, $[\{WCl_4(NNPh_2)\}_2]$.[47] The Ph_2PN complex **1** proved to be very oxygen sensitive in both solution and in the solid state. The IR spectrum showed a strong peak at 1439 cm^{-1} which is attributed to a ν_{P-Ph} stretching frequency.[24] There is a second strong peak at 1131 cm^{-1} which is attributed to a stretching frequency associated with the W–N–P unit.[46] The general similarity of the IR spectra to that observed for complexes **2** and **3** (discussed below) suggests that the complex is not a polymer linked together *via* the Ph_2P groups (Fig. 1(B)), although in the absence of a structure this possibility cannot be eliminated entirely.

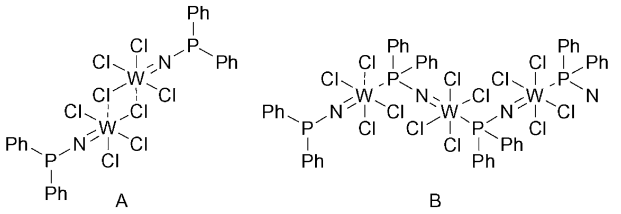

Fig. 1 Proposed structure of $[WCl_4(NPPh_2)]$ (A) and possible polymeric structure of $[WCl_4(NPPh_2)]$ complex (B).

It was hoped that if an additional ligand could be introduced into the coordination sphere the stability of the complexes could be increased. The reaction of **1** with PMe_2Ph gave a dark red complex **2** (Fig. 2) which had an elemental analysis consistent with the formulation $[WCl_4(NPPh_2)(PMe_2Ph)]$. The ^1H NMR (CD_2Cl_2) of this complex showed the expected protons in the aromatic region as a multiplet between 7.2 and 7.8 ppm. The ^{31}P NMR (CD_2Cl_2) showed two singlets, one at 37 ppm which

Table 1 Crystallographic data for the X-ray crystal structures of **4**, **5**, $ReOBr_3(PPh_3)_2$, L^2H, **6** and **7**

Compound	**4**	**5**	$ReBr_3(MeCN)(PPh_3)_2$[a]	L^2H[b]	**6**	**7**[c]
Chemical formula	$C_{58}H_{55}Cl_2N_5OP_3Re$	$C_{52}H_{46}Br_2N_2OP_3Re\cdot x$MeCN ($x \approx 0.7$)	$C_{38}H_{33}Br_3NP_2Re$	$C_{14}H_{17}N_2P$	$C_{19}H_{21}Cl_2N_2PTi$	$C_{24}H_{31}Cl_2N_2PRu$
Formula weight	1188.14	1182.94	991.55	244.28	427.17	550.47
Crystal system	Monoclinic	Monoclinic	Orthorhombic	Orthorhombic	Triclinic	Orthorhombic
Space group	$P2_1/n$	$P2_1/n$	*Pbca*	*Pbca*	$P\bar{1}$	*Pbca*
a/Å	18.6983(7)	15.2069(2)	10.2052(2)	16.4464(4)	9.3008(2)	18.7070(4)
b/Å	13.3095(5)	13.4521(2)	15.3009(3)	8.4807(2)	9.5959(2)	13.7367(3)
c/Å	21.6881(9)	24.6870(3)	23.1420(4)	19.3755(4)	12.3168(2)	18.8545(5)
α/°	90	90	90	90	67.4001(7)	90
β/°	90.6690(16)	105.5875(4)	91.8367(7)	90	77.4316(7)	90
γ/°	90	90	90	90	87.2789(8)	90
V/Å^3	5395.14(86)	4864.35(11)	3611.74(12)	2702.44(11)	989.74(3)	4845.1(2)
Z	4	4	4	8	2	8
μ/mm^{-1}	2.485	4.281	6.800	0.184	0.787	0.948
Reflections measured	28344	53221	44168	19242	17856	31161
R_{int}	0.086	0.071	0.074	0.048	0.031	0.081
Goodness of fit	1.0666	1.0987	1.1000	1.0875	1.0768	1.1166
R	0.0535	0.0325	0.0318	0.0358	0.0293	0.0295
$wR[I > 3\sigma(I)]$	0.0583	0.0352	0.0350	0.0410	0.0336	0.0306

[a] The compound is isostructural with the Cl analogue[50,51] and with the analogous Os complex.[61] [b] The NH hydrogen atom was located in a difference Fourier map and its coordinates and isotropic thermal parameter subsequently refined. Other hydrogen atoms were positioned geometrically after each cycle of refinement. [c] The NH hydrogen atom was located in a difference Fourier map and its coordinates and isotropic thermal parameter subsequently refined. Other hydrogen atoms were positioned geometrically after each cycle of refinement.

Table 2 Crystallographic data for the X-ray crystal structures of **8**, **9**, **10**, **12** and $[RuCl_2(\eta^6\text{-}p\text{-}MeC_6H_4{}^iPr)(PPh_2NHNHMe_2)]^+Cl^-$

Compound	**8**[a,b,c]	**9**[a]	**10**[a]	**12**[a]	$[RuCl_2(\eta^6\text{-}p\text{-}MeC_6H_4{}^iPr)(L^2H_2)]^+Cl^-\cdot THF$[a]
Chemical formula	$C_{28}H_{38}Cl_4N_3PRu$	$C_{28}H_{37}Cl_4N_2PRu$	$C_{24}H_{31}BClF_4N_2PRu$	$C_{28}H_{37}BCl_3F_4N_2PRu$	$C_{28}H_{40}Cl_3N_2OPRu$
Formula weight	690.48	675.47	601.82	726.82	659.04
Crystal system	Orthorhombic	Monoclinic	Orthorhombic	Monoclinic	Monoclinic
Space group	$P2_12_12_1$	$P2_1/n$	$Pna2_1$	$C2/c$	$P2_1/c$
a/Å	7.4308(2)	10.0630(2)	14.7058(5)	29.8867(4)	9.5016(2)
b/Å	13.7935(2)	14.6827(3)	16.8368(5)	10.3937(2)	20.4988(3)
c/Å	29.5131(4)	20.0092(5)	10.5355(4)	23.4925(4)	15.5874(2)
β/°	90	91.8167(9)	90	121.4595(7)	95.2880(7)
V/Å^3	3025.00(10)	2954.91(11)	2608.57(15)	6224.88(19)	3023.06(9)
Z	4	4	4	8	4
μ/mm^{-1}	0.948	0.967	0.809	0.859	0.860
Reflections measured	23307	22074	18147	31308	34647
R_{int}	0.046	0.054	0.054	0.055	0.034
Goodness of fit	1.0803	1.1084	1.1040	1.1179	1.0780
R	0.0398	0.0308	0.0343	0.0359	0.0282
$wR\,[I > 3\sigma(I)]$	0.0438	0.0340	0.0367	0.0409	0.0321

[a] The NH hydrogen atom was located in a difference Fourier map and its coordinates and isotropic thermal parameter subsequently refined. Other hydrogen atoms were positioned geometrically after each cycle of refinement. [b] The refined thermal parameters of the C and Cl atoms of the solvent were extremely large and highly anisotropic, indicative of disorder. This was modelled as disorder over two nearly-overlapping orientations. Coordinates, isotropic thermal parameters and site occupancies were refined for the disordered C and Cl atoms. Geometric restraints were applied: the C–Cl bond lengths were restrained to 1.78(2) Å and the Cl–C–Cl angles to 112(2)°. [c] Refinement of the Flack enantiopole parameter gave a value of 0.05(4), indicating that the crystal consisted predominantly of a single enantiomer[73] despite the lack of inherent chirality of the complex.

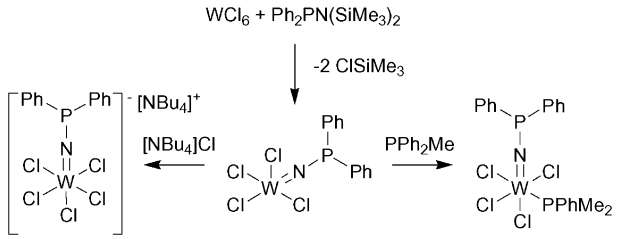

Fig. 2 Reaction scheme for the formation of the tungsten complexes.

is attributed to the $NPPh_2$ ligand and the second at 29 ppm which corresponds to the PMe_2Ph ligand. P–P coupling is not observed in the $^{31}P\{^1H\}$ NMR spectrum. The IR spectrum of the complex showed two distinctive bands analogous to those seen for **1**, slightly shifted to lower frequencies at 1436 and 1125 cm^{-1}. Despite repeated attempts in a variety of media, no mass spectra could be obtained using ES, MALDI or FAB techniques.

Reaction of **1** with $[NBu_4]Cl$ in dry dichloromethane (Fig. 2) resulted in the formation of a dark purple complex, **3**, with an elemental analysis consistent with $[WCl_5(NPPh_2)][NBu_4]$. As observed for the other tungsten complexes, two bands were observed in the IR at 1438 cm^{-1} and 1127 cm^{-1}. Despite repeated attempts, no $^{31}P\{^1H\}$ NMR signals could be observed and all ^1H NMR spectra showed very broad peaks. This may be due to a paramagnetic tungsten(v) impurity such as $[WCl_5(NHPPh_2)][NBu_4]$ which arises from reduction and protonation of **1**. Attempts to obtain $^{13}C\{^1H\}$ NMR and to carry out further reactions on these complexes was thwarted by their instability in solution.

Reaction of WCl_6 with more than one equivalent of the $Ph_2PN(SiMe_3)_2$ ligand only resulted in the formation of **1** with no evidence for a bis complex analogous to those known for the isodiazene system with tungsten (*e.g.* $[WCl_2(NNR_2)_2L_2]$ where R = Ph and L = 1,2-dimethoxyethane).[48]

Several variants of the $R_2PN(SiMe_3)_2$ proligand (R = ^{t}Bu, ^{i}Pr) were prepared. The complexation reactions showed the same dark blue colouration on initial reaction with WCl_6, but rapid decay to dark brown and then purple/blue solutions then occurred, and no meaningful analysis was obtained. P(v) analogues of the type $Ph_2P(X)N(SiMe_3)_2$ (X = O or S) were also prepared but again reactions with the tungsten starting materials gave a mixture of products which could not be separated or analysed.

Unfortunately no X-ray suitable crystals of the tungsten complexes could be obtained. Thus in order to gain some insight into the bonding in these complexes Density Functional (DF) calculations were carried out on **3** using the Gaussian 98W suite of programs.[27] Fig. 3 shows representations of the HOMO and LUMO orbitals obtained from the calculations while Fig. 4 shows the 2nd and 3rd highest occupied orbitals.

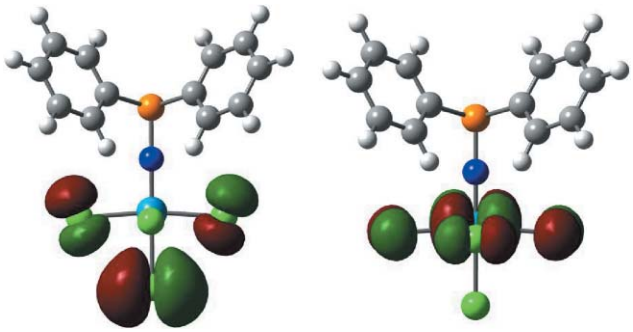

Fig. 3 DFT model of **3** (HOMO on the left and LUMO on the right).

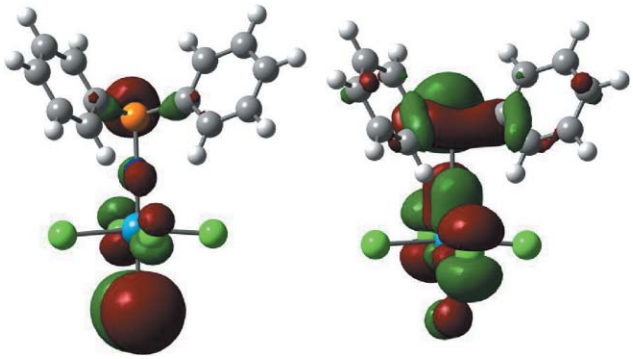

Fig. 4 DFT model of **3** (2nd highest occupied orbital on the left and 3rd highest occupied orbital on the right).

The calculations suggested a W–N bond distance of 1.756 Å and a N–P bond length of 1.701 Å which are typical lengths for a W=N double bond and a P–N single bond, respectively.[49,46] The Cl–W–N–P unit was predicted to be virtually linear with an N–W–Cl bond angle of 179.83°, and a P–N–W angle of

171.77°. The compound has a plane of symmetry running through P–N–W and the Ph_2PN ligand shows evidence of a strong *trans* influence as the W–Cl bond *trans* to the ligand has a calculated bond length 3.5% longer (2.486 Å) than the average W–Cl bond length in the equatorial plane (2.402 Å). The HOMO and LUMO orbitals have no contribution from the phosphazene ligand and involve non-bonding electron pairs on the halogen ligands. The second highest occupied orbital showed the P(III) lone pair and an anti-bonding W–Cl orbital *trans* to the phosphazene ligand. The third highest MO clearly shows the π-bonding component of the W–N multiple bond, consistent with the short W–N distance of 1.756 Å. There was also evidence for P–C antibonding orbitals on the P(III) atom, but these were not extended towards the nitrogen and there was no evidence for any P–N multiple bonding. This may well account for the observed instability of these complexes.

Rhenium phosphorylketimido complexes

Reaction of the $Ph_2PN(SiMe_3)_2$ proligand with $[ReOCl_3(PPh_3)_2]$ in MeCN under reflux resulted in the formation of a dark green crystalline material **4** in 10% yield on cooling (method A). Addition of two equivalents of PPh_3 to the reaction mixture improved the yield of the green crystalline material to around 40%. Further material could be obtained from the filtrate but was contaminated with the other orange product of this reaction which is identified from its X-ray crystal structure as the known complex $[ReCl_3(MeCN)(PPh_3)_2]$.[50,51] The analogous reaction of the proligand with $[ReOBr_3(PPh_3)_2]$ gave **5** and $[ReBr_3(MeCN)(PPh_3)_2]$.

The X-ray crystal structure of 4

The crystals deposited directly from the reaction mixture proved suitable for an X-ray structure determination (details in Table 1). An ORTEP representation of the structure appears in Fig. 5 and selected bond lengths and angles appear in Table 3. The geometry about the rhenium centre is pseudo-octahedral with previously unknown phosphorylketimido ligand –N=C(CH_3)–P(O)Ph_2) bound *trans* to one chloride and the two triphenylphosphine ligands bound *trans* to each other. The Re–Cl distances are virtually identical and suggest that the ketimide ligand exerts a similar *trans* influence to that of MeCN. The length of the Re(1)–N(1) bond at 1.809(7) Å, combined with the Re(1)–N(1)–C(1) bond angle of 176.6° is consistent with a double bond (*cf*. *trans*-

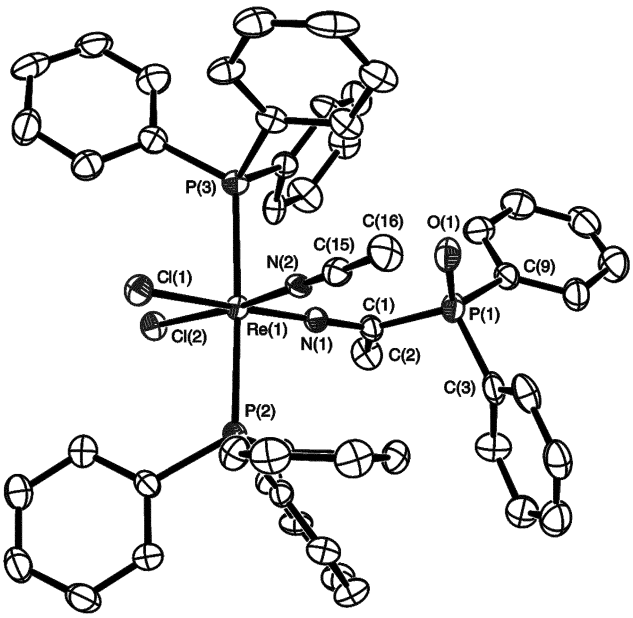

Fig. 5 ORTEP view (40% probability ellipsoids) of the X-ray crystal structure of **4** with hydrogen atoms omitted for clarity.

Table 3 Selected bond lengths (Å) and angles (°) for **4**

Re(1)–Cl(1)	2.4637(19)	N(1)–C(1)	1.27(1)
Re(1)–Cl(2)	2.4123(18)	C(1)–C(2)	1.552(11)
Re(1)–N(1)	1.809(7)	C(1)–P(1)	1.801(8)
Re(1)–N(2)	2.049(6)	P(1)–O(1)	1.489(6)
Re(1)–P(2)	2.434(2)	P(1)–C(3)	1.80(1)
Re(1)–P(3)	2.4284(19)	P(1)–C(9)	1.806(9)
Cl(1)–Re(1)–Cl(2)	90.88(7)	N(1)–Re(1)–P(2)	91.8(2)
Cl(1)–Re(1)–N(1)	170.3(2)	Cl(1)–Re(1)–P(3)	91.06(7)
Cl(2)–Re(1)–N(1)	98.6(2)	N(1)–Re(1)–P(3)	91.0(2)
Cl(1)–Re(1)–N(2)	79.01(18)	P(2)–Re(1)–P(3)	177.13(7)
Cl(2)–Re(1)–N(2)	169.80(18)	Re(1)–N(1)–C(1)	176.6(6)
N(1)–Re(1)–N(2)	91.5(3)	N(1)–C(1)–C(2)	120.1(7)
Cl(1)–Re(1)–P(2)	86.08(6)	C(2)–C(1)–P(1)	123.1(6)

$[Re(OH)(N{=}CMe_2)(dppe)_2][HSO_4]$, for which Re–N = 1.901(5) and Re–N–C = 178.9(5)°).[52] The C(1)–N(1) bond length is also consistent with a double bond at 1.27(1) Å. The carbon C(1) is sp^2 hybridised with an N(1)–C(1)–P(1) angle of 116.8° and an N(1)–C(1)–C(2) angle of 120.9°. These bond distances and angles are similar to those seen in other ketimido complexes {*e.g.* $[(C_5H_5)(Bu^t_2C{=}N)TiMe_2]$}[53,54] and the distances and angles around the phosphorus are typical for a phosphine oxide.[55] The bromo analogue **5** was found to be essentially isostructural and its details are not discussed here.

Electrospray mass spectrometry of **4** in CH_2Cl_2 showed an ion of 100% relative abundance at m/z 1024, which corresponds to the species formed by protonation and loss of MeCN. In the case of the bromide complex, **5**, the FAB^+ mass spectrum showed a peak at m/z 1033 (100%) and one at 1074 (40%) which corresponds to the cations formed by the loss of both Br^- and MeCN or only Br^-, respectively. The $^{31}P\{^1H\}$ NMR spectrum (in CD_2Cl_2) of **4** shows two singlets at −11 and +6 ppm. The resonance at −11 ppm is due to the two equivalent PPh_3 ligands (*cf.* ^{31}P NMR for $[Re(NPh)Cl_3(PPh_3)_2]$ at −19 ppm in $CDCl_3$)[56,57] and the resonance at 6 ppm is due to the P(V) in the $NC(CH_3)P(O)Ph_2$ ligand [*cf.* $Ph_2PN(SiMe_3)_2$ at 50.2 ppm].[22] The $^{31}P\{^1H\}$ NMR spectrum of **5** shows the same peaks slightly shifted to −17 and +4 ppm assigned as before. The IR spectra of complexes **4** and **5**, showed bands due to $\nu_{C=N}$ at 1541 cm^{-1} and 1542 cm^{-1}, respectively.[58] It was not possible to obtain elemental analysis of either complex **4** or **5** due to the co-crystallization with $[ReCl_3(MeCN)(PPh_3)_2]$ or $[ReBr_3(MeCN)(PPh_3)_2]$, respectively.

A proposed mechanism for the formation of complexes **4** and **5** is shown in Fig. 6. Acetonitrile appears essential as

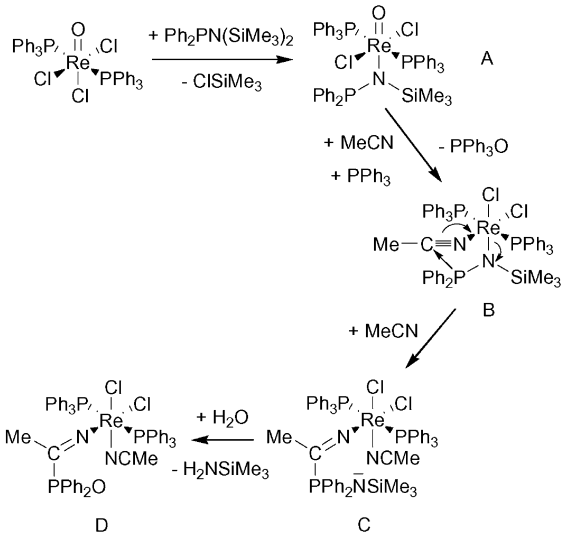

Fig. 6 Proposed mechanism for the formation of the phosphorylketimide ligand.

the use of other solvents (THF or toluene) led to brown solutions, and no clean products could be isolated. It is known that $[ReOCl_3(PPh_3)_2]$ reacts irreversibly with acetonitrile and triphenylphosphine to give $[ReCl_3(MeCN)(PPh_3)_2]$ and this appears to be in competition with the formation of **4** since the Re(III) acetonitrile complex does not react with $Ph_2PN(SiMe_3)_2$ to give complex **4**. The chloride *trans* to the oxo group is more labile due to the higher *trans* effect of the oxo group and will be readily replaced through elimination of trimethylchlorosilane to gives species **A**.

Reduction of the rhenium–oxo group by triphenylphosphine and coordination of MeCN to the coordinatively unsaturated Re(III) species formed produces **B**. The acetonitrile ligand in $[ReCl_3(MeCN)(PPh_3)_2]$ is known to be susceptible to nucleophilic attack, and so it is possible that intramolecular nucleophilic attack by P at the nitrile carbon can then occur as shown in species **B**, giving **C**.[59,60] However, this requires that the $N(SiMe_3)PPh_2$ ligand be *cis* to the nitrile ligand, otherwise intramolecular attack is not possible. Finally, hydrolysis of the negatively charged phosphinamine group gives species **D**.

Attempts to verify the proposed mechanism by a variety of spectroscopic techniques was not successful, furthermore, the reaction of one of the possible hydrolysis products of the ligand, $Ph_2P(O)H$, with $[ReCl_3(MeCN)(PPh_3)_2]$ does not yield **4**. However, the mechanism is consistent with the observation of two products and the known chemistry of these systems.

Phosphinohydrazine and phosphinohydrazido ligands

All attempts to prepare early and middle transition metal complexes of phosphazenido (R_2P–NR', R = Ph, R′ = Ph, Me, cyclohexyl) ligands were unsuccessful in our hands. Reaction of R_2PNHR with appropriate metal halides in the presence of a range of bases at various temperatures and in several different solvents gave intractable mixtures. Complexes of $[Ph_2P$–N–$PPh_2]$ with Ti(IV) and Zr(IV) are known[19,20] and we investigated the effect of replacing one PPh_2 with an NR_2 group on the coordination geometry of the complexes, with the possibility of P–N, or N–N donation and the formation of three- or four-membered chelate rings (Fig. 7).

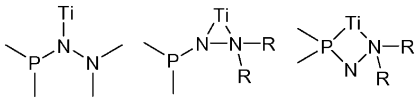

Fig. 7 Possible phosphinohydrazido ligand binding modes.

$Ph_2PNHNMe_2$ was first produced by Sisler *et al.* in 1966, and subsequently used as a neutral phosphorus donor with several metals.[23,24] The synthesis involves reaction of PPh_2Cl with two equivalents of NH_2NMe_2 producing the desired ligand PPh_2NHNMe_2, L^2H (Fig. 8) and the HCl salt of the hydrazine, (the use of Et_3N as a base yields only $(PPh_2)_2NNMe_2$ and the HCl salt of the hydrazine, presumably due to the lower solubility in Et_2O of the hydrazine hydrochloride compared to $[Et_3NH]^+Cl^-$). In contrast the new ligands L^3H and L^4H (Fig. 8) were both prepared through reaction of one equivalent of each of the respective hydrazine, Ph_2PCl and Et_3N in Et_2O. On removal of the $Et_3NH^+Cl^-$ by filtration and evaporation of the solution to dryness, the two ligands were obtained pure as colourless oils in quantitative yield. They are all soluble and stable in dry, degassed toluene, benzene, CH_2Cl_2, $CHCl_3$, Et_2O, pentane and hexane. The ^1H NMR spectra (in CD_2Cl_2 or $CDCl_3$) of L^2H, L^3H and L^4H showed a doublet at 3.31 ($^2J_{H-P} = 12$ Hz), 3.35 ($^2J_{H-P} = 10$ Hz) and 3.25 ppm ($^2J_{H-P} = 8$ Hz), respectively, attributed to NH. The $^{31}P\{^1H\}$ NMR spectra of the three ligands showed a single resonance at 38.6, 39.2 and 35.6 ppm.

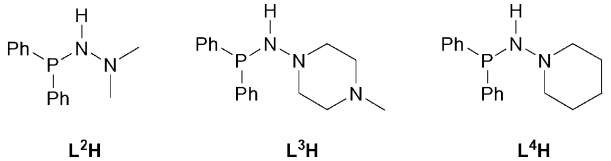

Fig. 8 Phosphinohydrazine ligands.

The $^{31}C\{^1H\}$ NMR spectra were unambiguously assigned using ^1H–^{13}C HMQC and ^1H–^1H COSY experiments and showed doublets in the aromatic region due to ^{13}C–^{31}P coupling, with coupling constants similar to those previously reported for Ph_3P.[62] The $N(CH_3)_2$ carbon resonances are also split due to ^{13}C–^{31}P coupling, with a coupling constant of about 4 Hz as expected for a three-bond aliphatic coupling.[63] The *ipso*-carbon resonances were not observed. It was not possible to obtain a mass spectrum of either L^3H or L^4H, however the ES^+ MS for L^2H showed $[L + H]^+$ as the major peak and suitable elemental analyses were obtained for all three. The IR spectrum of L^2H was published by Sisler *et al.* showing strong peaks at 1432 cm^{-1} (ν_{P-Ph}), 1583 cm^{-1} (ν_{N-H}) and 740 cm^{-1} (ν_{N-P}). Unsurprisingly, the new ligands L^3H and L^4H have very similar IR spectra showing the same characteristic peaks.

Recrystallisation of L^2H from hot hexane produced crystals suitable for X-ray analysis (Fig. 9, Tables 1 and 4). The NH group projects towards the terminal N of a neighbouring molecule, but the N···N distance $(N(1)\cdots N(2)' = 3.396(2)$ Å, symmetry operator $1/2 - x, -1/2 + y, z)$ is greater than that generally associated with N···N hydrogen bonds. The coordination geometry around N(1) is considerably flatter than is normal for a secondary amine (P(1)–N(1)–N(2) = 115.50(10)°), which, together with the short N–P bond length (1.6815(13) Å), suggests that there is an interaction between the N lone pair and the P atom giving some multiple bond character.

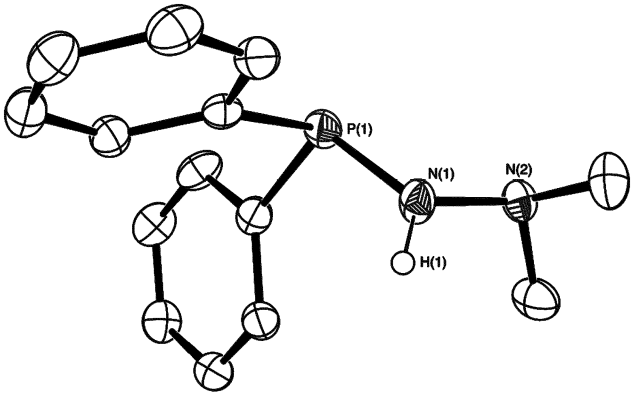

Fig. 9 ORTEP view (40% probability ellipsoids) of the X-ray crystal structure of L^2H with geometrically positioned hydrogen atoms omitted for clarity.

Phosphorus(III) hydrazine and hydrazide complexes

In the limited number of complexes published containing the ligand L^2H,[64–66] none have contained it as an anionic ligand. However, reaction of two equivalents of L^2H with $[(C_5H_5)TiCl_3]$ in Et_2O produced $[Ph_2PNHNHMe_2]^+Cl^-$ and the relatively air- and moisture-stable complex $[(C_5H_5)TiCl_2(Ph_2PNNMe_2)]$ **6** in high yield. Complete separation of the HCl salt of the ligand and the complex proved difficult as they have very similar solubility in a wide range of solvents, however, filtering the Et_2O solution at −18 °C proved successful.

The $^{31}P\{^1H\}$ NMR spectrum of **6** ($CDCl_3$) showed a single resonance at 55.8 ppm. In the ^1H NMR spectrum, the NH peak of the free ligand (observed at 3.31 ppm) is missing and the peak at 2.46 ppm, assigned to $N(CH_3)_2$ has shifted to 3.10 ppm. The C_5H_5 resonance has also shifted, from 7.0 ppm[67] in $[(C_5H_5)TiCl_3]$ to 6.19 in the complex **6**. As in the free ligand, the resonances corresponding to the *ortho*- and *meta*-carbons in the $^{31}C\{^1H\}$ NMR spectrum of the complex were split due coupling to ^{31}P

Table 4 Selected bond lengths (Å) and angles (°) for L^2H, **7**, **8**, **9**, **10**, **12** and $[RuCl_2(\eta^6\text{-}p\text{-}MeC_6H_4{}^iPr)(L^2H_2)]^+Cl^-$

	L^2H	**7**	**8**	**9**	**10**	**12**	$[RuCl_2(\eta^6\text{-}p\text{-}MeC_6H_4{}^iPr)(L^2H_2)]^+Cl^-$
Ru(1)–P(1)	—	2.3238(8)	2.3222(12)	2.3425(8)	2.3133(9)	2.3109(9)	2.3379(5)
Ru(1)–Cl(1)	—	2.4122(9)	2.4235(11)	2.4167(8)	2.3918(11)	2.3901(9)	2.4215(5)
Ru(1)–Cl(2)	—	2.4103(9)	2.4097(11)	2.4120(8)	2.221(4)[e]	2.227(3)[e]	2.4163(5)
Ru(1)–cymene[a]	—	1.69	1.70	1.70	1.72	1.73	1.71
P(1)–N(1)	1.6815(13)	1.673(3)	1.691(4)	1.664(3)	1.658(4)	1.665(3)	1.7017(18)
N(1)–N(2)	1.4388(17)	1.433(4)	1.432(5)	1.434(4)	1.457(5)	1.444(4)	1.443(2)
N(2)–C(1)	1.455(2)	1.457(5)	1.453(6)	1.467(4)	1.480(6)	1.505(4)	1.495(3)
N(2)–C(X)	1.457(2)[b]	1.466(5)[b]	1.479(6)[c]	1.473(4)[d]	1.484(6)[b]	1.508(5)[d]	1.494(3)[a]
N(1)–H(1)	0.88(2)	0.80(4)	0.86(6)	0.86(5)	0.89(6)	0.81(5)	0.90(3)
N(2)–H(2)	—	—	—	—	—	—	0.90(3)
Ru(1)–P(1)–N(1)	—	112.96(11)	112.09(15)	111.30(11)	88.24(13)	88.48(12)	114.58(7)
Ru(1)–N(2)–N(1)	—	—	—	—	97.2(2)	97.67(19)	—
P(1)–Ru(1)–N(2)	—	—	—	—	66.79(10)	66.75(8)	—
P(1)–N(1)–N(2)	115.50(10)	116.9(2)	117.0(3)	117.7(2)	106.4(3)	106.7(2)	119.60(14)
N(2)–N(1)–H(1)	114.1(13)	112(3)	114(4)	117(3)	119(3)	123(4)	108.2(18)
N(1)–N(2)–C(1)	107.98(12)	109.2(3)	110.4(4)	110.3(2)	108.3(4)	111.4(3)	113.54(18)
N(1)–N(2)–C(X)	111.17(12)[b]	110.3(3)[b]	109.1(3)[c]	108.8(2)[d]	109.0(3)[b]	109.8(3)[d]	108.18(18)[b]
C(1)–N(1)–C(X)	110.90(14)[b]	110.8(3)[b]	108.9(4)[c]	111.2(2)[d]	108.4(4)[b]	108.0(3)[d]	111.64(18)[b]

[a] Distance from Ru(1) to the best plane of the C_6 ring. [b] X = 2. [c] X = 3. [d] X = 5. [e] Length of Ru(1)–N(2) bond, not Ru(1)–Cl(2).

($^2J_{C-P} = 20$ and $^3J_{C-P} = 6$ Hz, respectively, which are consistent with literature values).[62] The $N(CH_3)_2$ carbons appeared as a doublet due to three-bond coupling to ^{31}P, and not due to the slight asymmetry seen in the crystal structure. This was confirmed by running the $^{13}C\{^1H\}$ NMR spectrum at both 300 and 500 MHz, with both spectra showing a peak to peak separation of 10.4 Hz, which is consistent with ^{31}P coupling and not magnetic inequivalence.

Despite numerous attempts, it was not possible to obtain a mass spectrum of the complex. However, on standing, the Et_2O solution produced a large number of orange crystals suitable for X-ray crystallography (Fig. 10). The structure is similar to the previously reported $[(C_5H_5)TiCl_2(NMe_2NMe)]$,[68] (Table 5) however, the two Ti–N bond lengths are slightly less asymmetric, with Ti–NMe_2 at 2.1689(15) Å and Ti–NP at 1.9013(14) Å [*cf.* 2.217 and 1.849 Å, respectively, for $[(C_5H_5)TiCl_2(NMe_2NMe)]$. The N–N bond shows no multiple bonding character (bond length = 1.4337(19) Å, and similarly, the P–N bond length (1.7319(14) Å) is characteristic of a single bond.[69] As expected, the soft P lone pair does not coordinate to the hard Ti centre, and the lone pair is directed away from the Ti metal centre. The IR spectrum of the complex showed bands at 1434 cm^{-1} (s, ν_{P-Ph}) and 742 cm^{-1} (s, ν_{P-N}), similar to the spectrum of the free ligand.

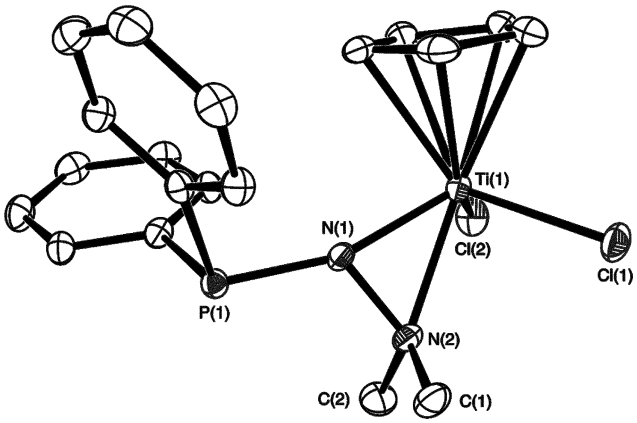

Fig. 10 ORTEP view (40% probability ellipsoids) of the X-ray crystal structure of **6** with hydrogen atoms omitted for clarity.

The NH peak, observed at 1583 cm^{-1} in the IR spectrum of the free ligand is missing as expected.

Density functional (DF) calculations were carried out on **6** in order to compare the optimised geometry with the X-ray crystal structure, and to confirm the accuracy of the model chosen

Table 5 Selected bond lengths (Å) and angles (°) for **6**, the DF optimised structure of **6** and $(Cp)TiCl_2(NMe_2NMe)$.[68]

	6	DFT Calc.	Δ[a]	$[(Cp)TiCl_2(NMe_2NMe)]$
Ti(1)–N(1)	1.9013(14)	1.917	+0.79	1.849[b]
Ti(1)–N(2)	2.1689(15)	2.224	+2.54	2.217[c]
Ti(1)–Cl(1)	2.3270(5)	2.317	−0.43	2.329[d]
Ti(1)–Cl(2)	2.3165(5)	2.312	−0.17	
Ti(1)–(C_5H_5)[d]	2.3728	2.400	+1.15	2.352
N(1)–N(2)	1.4337(19)	1.424	−0.70	1.412
P(1)–N(1)	1.7319(14)	1.751	+1.10	
Ti(1)–N(1)–P(1)	161.83(9)	159.93	−1.17	154.90[e]
Ti(1)–N(1)–N(2)	79.79(9)	82.03	2.80	84.57
Ti(1)–N(2)–N(1)	59.63(8)	58.63	−1.68	56.10
N(1)–Ti(1)–N(2)	40.58(5)	39.34	−3.06	39.33
N(2)–N(1)–P(1)	117.90(11)	117.97	0.06	120.53[f]
Ti(1)–N(2)–C(1)	120.49(12)	124.06	2.96	122.93
Ti(1)–N(2)–C(2)	125.60(12)	121.72	−3.09	122.93
C(1)–N(1)–C(2)	111.14(15)	110.65	−0.44	112.15

[a] Δ = {(Calc. value − X-ray value)/X-ray value} × 100%. [b] Ti–NMe bond length. [c] Ti–NMe_2 bond length. [d] Average bond length. [e] Ti–N–C, not Ti–N–P bond angle. [f] N–N–C, not N–N–P bond angle.

for representing such P–N complexes. As before, the Gaussian 98W[27] suite of programs was used. The optimised bond lengths (Table 5) show that the optimised structure is in good agreement with that determined by X-ray crystallography. The calculated structure generally slightly overestimates the bond lengths by about 0.75%, up to a maximum of 2.5% for the Ti(1)–N(2) bond. The HOMO orbital is delocalised over the Ti–N(1)–P–C(*ipso*) unit, but also has some phosphorus lone pair character, and the LUMO is an anti-bonding M–Cl orbital. This is in comparison to $[(C_5H_5)TiCl_2(MeNNMe_2)]$, for which the HOMO is a Ti–(C_5H_5) bonding orbital (for **6**, the second and third highest occupied orbitals are Ti–(C_5H_5) bonding in character), and the LUMO, which is an anti-bonding M–Cl orbital, as for **6**.

Unfortunately, it was not possible to mimic the above reaction with either L^3H or L^4H. Reaction of two equivalents of L^3H with $[(C_5H_5)TiCl_3]$ gave a $^{31}P\{^1H\}$ NMR spectrum showing at least five ^{31}P environments. The main peaks (from integration) were two doublets at 35.9 and −22.7 ppm ($^1J_{P-P} = 227$ Hz) which were tentatively assigned to $Ph_2P–P(=N–R)Ph_2$ [*cf.* $Ph_2P–P(=O)Ph_2$ at 34 and −23 ppm, $^1J_{P-P} = 220$ Hz[70] and $Ph_2P–P(=N–PyH^+)Ph_2$ at 18.9 and −20.3 ppm, $^1J_{P-P} = 280$ Hz],[71] showing the instability of the P–N bond to hydrolysis. Reaction of L^4H gave very similar results with peaks at 35.4 and −23.4 ppm ($^1J_{P-P} =$ 226 Hz) in the $^{31}P\{^1H\}$ NMR spectrum. In the presence of Et_3N as base, the reaction produces a crystalline red solid, however, the high air- and or moisture-sensitivity of this product has precluded any meaningful analysis. The difference in stability of the Ti complex of L^2H as opposed to that of the large array of other $R^1{}_2P–NR^2$ compounds that we have investigated including those of L^3H and L^4H is put down to the ability of the sterically small ligand L^2H to bind to the Ti centre through both of its N atoms (Fig. 7). However, that is obviously not possible for the diarylphosphazene ligands, and is not possible for L^3H and L^4H due to the steric requirements of the cyclohexyl ring, thus reducing the strength of the bonding interactions between the ligand and the metal, and so increasing the ease of hydrolysis of the complexes.

In contrast to the above reaction of L^2H with $[(C_5H_5)TiCl_3]$, the reaction of four equivalents of L^2H with $[\{RuCl(\mu\text{-}Cl)(\eta^6\text{-}p\text{-}MeC_6H_4{}^iPr)\}_2]$ in THF gave a product with L^2H bound *via* only the phosphorus. In fact, reaction of two equivalents of L^2H with $[\{RuCl(\mu\text{-}Cl)(\eta^6\text{-}p\text{-}MeC_6H_4{}^iPr)\}_2]$ gave the complex $[RuCl_2(\eta^6\text{-}p\text{-}MeC_6H_4{}^iPr)(L^2H)]$ (**7**) in good yield (77%). The ^1H NMR spectrum of the complex showed that the NH proton chemical shift had moved downfield to 3.95 ppm, and the $^1H–^{31}P$ coupling constant had increased to 30 Hz (from 12 Hz in L^2H). The $^{31}P\{^1H\}$ NMR spectrum shows a single resonance at 65.7 ppm (*cf.* 38.6 ppm for the free ligand) consistent with a Ru–P(III) complex.[72] As in the free ligand and the Ti complex, the $^{13}C\{^1H\}$ NMR spectrum shows $^{13}C–^{31}P$ coupling with J values comparable with the literature.[62] The aromatic $\eta^6\text{-}p\text{-}MeC_6H_4{}^iPr$ CH carbon atoms also appear as doublets due to coupling to ^{31}P through the metal centre, with $^2J_{C-P}$ values of approximately 5 Hz, and the analysis of HMQC and HMBC spectra allowed the unambiguous assignment of the two pairs of aromatic $\eta^6\text{-}p\text{-}MeC_6H_4{}^iPr$ CH protons. The ES^+ MS of the complex showed almost exclusively the desired compound, $[M + H]^+$ at m/z 551.5.

Slow evaporation of a THF solution of **7** under N_2 yielded crystals suitable of X-ray structure determination (Fig. 11, Tables 1 and 4). The phenyl ring of the $\eta^6\text{-}p\text{-}MeC_6H_4{}^iPr$ ligand is coordinated in a symmetric manner and the Ru atom lies 1.69 Å from the ring centroid. As with the free ligand, the coordination geometry around N(1) is considerably flatter than normal for a secondary amine, which together with an even shorter P(1)–N(1) bond length (1.673(3) Å) and a P(1)–N(1)–N(2) bond angle of 116.9(2)° suggests that there is some P(1)–N(1) multiple bond character. This is in contrast to the Ti complex which, as already discussed, has a P–N bond length characteristic of a single bond.

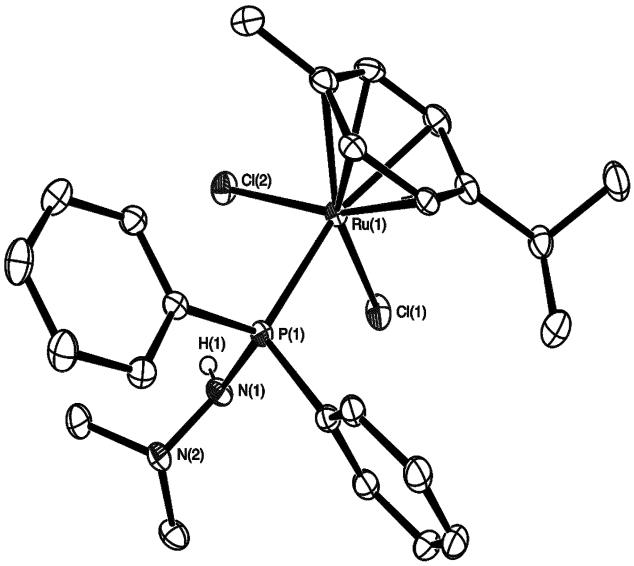

Fig. 11 ORTEP view (40% probability ellipsoids) of the X-ray crystal structure of **7** with geometrically positioned hydrogen atoms omitted for clarity.

Meanwhile the N–N bond lengths of the complexes **6** and **7** and the free ligand (L^2H) are almost exactly the same (1.4337(19), 1.433(4) and 1.4388(7) Å, respectively). The Ru(1)–P(1) bond length of 2.3238(8) Å is similar to that of previously reported compounds containing a Ru–P(III) bond.[72] The NH group does not participate in hydrogen bonding in the solid state, although this is probably as a result of its high degree of steric crowding.

Attempts to deprotonate the ligand in complex **7** were made using a variety of bases including KO^tBu, proton sponge, Et_3N, $NaNH_2$, NaOMe, however, the ^1H and $^{31}P\{^1H\}$ NMR spectra of the reaction solutions showed no change.

The reaction of L^3H and L^4H with $[\{RuCl(\mu\text{-}Cl)(\eta^6\text{-}p\text{-}MeC_6H_4{}^iPr)\}_2]$ produced complexes analogous to **7**. The $^{31}P\{^1H\}$ NMR spectra for both $[RuCl_2(\eta^6\text{-}p\text{-}MeC_6H_4{}^iPr)(L^3H)]$ **8** and $[RuCl_2(\eta^6\text{-}p\text{-}MeC_6H_4{}^iPr)(L^4H)]$ **9** showed resonances at *ca.* 65 ppm and ^1H NMR spectra showed NH resonances at *ca.* 4 ppm as anticipated (see Table 6). The $^{13}C\{^1H\}$ NMR spectra are also analogous to that seen for **7**, with $^{13}C–^{31}P$ coupling again evident. The ES^+ MS of both showed the peak corresponding to $[M]^+$, the elemental analyses are satisfactory and the IR spectra (KBr disc) of both have resonances at ~3300, ~1435 and ~745 cm^{-1}, assigned to ν_{N-H}, ν_{P-Ph} and ν_{P-N}, respectively.

Recrystallisation of **8** and **9** by layering a CH_2Cl_2 solution with pentane produced crystals suitable for X-ray analysis. The crystal structures of both of the complexes **8** and **9** are totally isostructural with that of **7** and so are not shown here and are not worthy of extensive discussion (selected bond lengths and angles can be found in Table 4, and details of the structure refinement in Table 2). The only significant differences are in the NH hydrogen bonding. In **8**, the NH group appears to be interacting with one of the Cl atoms of the same molecule. While both the N(1)···Cl(1) distance (3.211(4) Å) and the H···Cl distance (2.52(6) Å) are sufficiently short to suggest that there is an intramolecular hydrogen bond, the N–H···Cl angle is relatively acute (138(5)°) for a hydrogen bond. The crystal structure of **9** shows that the NH group approaches both Cl ligands of the same molecule relatively closely [N(1)···Cl(1) 3.410(3), N(1)···Cl(2) 3.129(3) Å]. However, the N–H···Cl angles are both below 120° suggesting no hydrogen bond is present. The crystal structures of both **8** and **9** show that the geometry of the protonated N atom (N(1)) is a flattened trigonal pyramid. This, together with the large P–N–N angle (117.0(3) and 117.7(2)°, respectively) and short P–N bond distance (1.691(4) and 1.664(3) Å, respectively) suggests that, as in complex **7**, the P–N bonds have partial multiple-bond character.

Table 6 $^{31}P\{^{1}H\}$ and selected ^{1}H NMR data for compounds $L^{2}H$, $L^{3}H$, $L^{4}H$ and **6–13**

Compound		Chemical shift/ppm	
		δ ^{31}P	δ NH ($^{2}J_{H-P}$/Hz)
$L^{2}H$	$Ph_2PNHNMe_2$	38.6[a]	3.31[a] (12)
$L^{3}H$	$Ph_2PNHNCH_2CH_2N(CH_3)CH_2CH_2$	39.2[b]	3.35[b] (10)
$L^{4}H$	$Ph_2PNHNCH_2CH_2CH_2CH_2CH_2$	35.6[b]	3.25[b] (8)
6	$(C_5H_5)TiCl_2(PPh_2NNMe_2)$	55.8[b]	—
7	$[RuCl_2(\eta^6\text{-}p\text{-}MeC_6H_4{}^{i}Pr)(L^{2}H)]$	65.7[b]	3.95[b] (30)
8	$[RuCl_2(\eta^6\text{-}p\text{-}MeC_6H_4{}^{i}Pr)(L^{3}H)]$	67.9[b]	4.10[b] (30)
9	$[RuCl_2(\eta^6\text{-}p\text{-}MeC_6H_4{}^{i}Pr)(L^{4}H)]$	66.4[b]	4.00[b] (31)
10	$[RuCl(\eta^6\text{-}p\text{-}MeC_6H_4{}^{i}Pr)(L^{2}H)]^{+}BF_4^{-}$	43.7[a]	7.35[a] (3)
11	$[RuCl(\eta^6\text{-}p\text{-}MeC_6H_4{}^{i}Pr)(L^{3}H)]^{+}BF_4^{-}$	46.9[a]	7.05[a] (3)
12	$[RuCl(\eta^6\text{-}p\text{-}MeC_6H_4{}^{i}Pr)(L^{4}H)]^{+}BF_4^{-}$	45.9[a]	7.01[a] (3)
13	$[(\eta^6\text{-}p\text{-}MeC_6H_4{}^{i}Pr)Cl_2Ru(\mu^2,\eta^3\text{-}Ph_2PNNMe_2)TiCl_2(C_5H_5)]$	86.3[a]	—

[a] Spectrum run in CD_2Cl_2. [b] Spectrum run in $CDCl_3$.

Cationic ruthenium phosphinohydrazine complexes

The reaction of **7** with $AgBF_4$ in toluene resulted in Cl^{-} ion abstraction from the Ru coordination sphere and the formation of a cationic Ru species $[RuCl(\eta^6\text{-}p\text{-}MeC_6H_4{}^{i}Pr)(L^{2}H)]^{+}BF_4^{-}$ **10**. The ES^{+} MS of the resulting orange solid showed the only significant peak to be due to $[M]^{+}$ as expected. The $^{31}P\{^{1}H\}$ NMR spectrum (CD_2Cl_2) of the compound showed a single peak at 43.7 ppm, and the ^{1}H NMR (CD_2Cl_2) also showed several distinct differences to that of the **7**. The spectrum showed inequivalent methyl protons of the $N(CH_3)_2$ and isopropyl groups. These inequivalencies are due to the formation of a chelate ring, which produced a chiral complex and so making the protons diastereotopic. The close approach of the $N(CH_3)_2$ group to one side of the $\eta^6\text{-}p\text{-}MeC_6H_4{}^{i}Pr$ ring restricts the rotation of the isopropyl group, and removes the magnetic equivalence of the two methyl groups of the *iso*-propyl group (as can be seen in the crystal structure, Fig. 12).

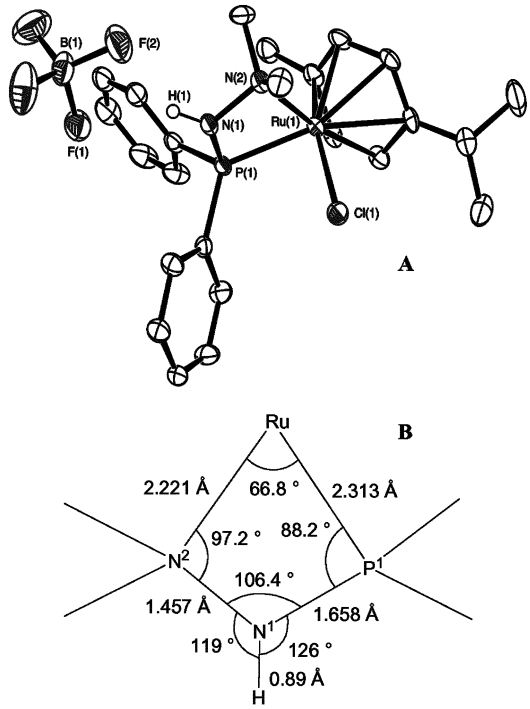

Fig. 12 ORTEP view (40% probability ellipsoids) of the X-ray crystal structure (A, with geometrically positioned hydrogen atoms omitted for clarity) and selected bond lengths and angles for **10** (B).

The NMR spectra in CD_3CN shows very different resonances to that in CD_2Cl_2. The phosphorus resonance in the $^{31}P\{^{1}H\}$ NMR spectrum in CD_3CN shifts to 70.8 ppm (*cf.* $L^{2}H$ at 38.9 ppm, **7** at 65.7 ppm, and **10** at 43.7 ppm, see Table 6). In the ^{1}H NMR spectrum, the two $N(CH_3)_2$ proton resonances are now coincident and appear at the same chemical shift as in **7**. It appears that solvation of the complex in MeCN results in coordination of at least one molecule of MeCN to the metal centre and so ring opening the four-membered metal chelate.

Recrystallisation of **10** by layering a CH_2Cl_2 solution with pentane produced crystals suitable for X-ray crystal structure analysis (Fig. 12, Tables 2 and 4). As expected, a chelate ring is formed in order to maintain 18-electron configuration at the Ru centre, and a four-membered ring is preferred over the two possible three-membered rings. This is the first example of a four-membered Ru–P–N–N metal chelate complex (Fig. 12(A)), which is a neutral analogue of the known ruthenium structure of the triazenido ligand $[Ru(N(R^{1})=N\text{–}N\text{–}R^{2})(PPr^{i}{}_3)Cl_3]$.[74] The phenyl ring of the $\eta^6\text{-}p\text{-}MeC_6H_4{}^{i}Pr$ ligand is coordinated in a symmetrical manner with the Ru atom lying 1.72 Å from the best plane of the C_6 ring. The sum of the internal angles of the Ru(1)–P(1)–N(1)–N(2) chelate ring is 358.63°, indicating that it is very close to planar in geometry (Fig. 12(B)). Similarly the sum of the bond angles around N(1) is 351.4°, which, combined with the short P(1)–N(1) bond of 1.658(4) Å is indicative of significant multiple bond character in the P–N bond. The P–Ru bond distance of 2.3133(9) Å is very similar to the neutral compound **7**. The NH group forms a bifurcated hydrogen bond to two of the F atoms of a neighbouring anion (N(1)···F(1) 2.954(5) Å and N(1)···F(2) 3.034(5) Å).

The reaction of **8** with $AgBF_4$ in toluene/benzene also results in Cl^{-} ion abstraction and the formation of a cationic Ru species which after rapid recrystallisation from CH_2Cl_2–E_2O produced $[RuCl(\eta^6\text{-}p\text{-}MeC_6H_4{}^{i}Pr)(L^{3}H)]^{+}BF_4^{-}$ **11**. The ES^{+} MS of the resulting ochre solid showed the expected peak at 570 m/z due to $[M]^{+}$. The $^{31}P\{^{1}H\}$ NMR spectrum (CD_2Cl_2) of the compound shows a single peak at $\delta = 46.9$ ppm and as for **10** the ^{1}H NMR showed inequivalent methyl protons of the *iso*-propyl group and inequivalent aromatic CH's for the two sides of the $\eta^6\text{-}p\text{-}MeC_6H_4{}^{i}Pr$ ring. This is presumably due to the coordination of a lone pair on one of the nitrogen atoms to the coordinatively unsaturated Ru centre forming a four- or seven-membered ring which locks the conformation of the $\eta^6\text{-}p\text{-}MeC_6H_4{}^{i}Pr$ ring. The complex is, however, unstable in solution in CH_2Cl_2, with after 24 h, over 75% of the sample decomposing, precluding any further meaningful analysis of the complex.

Reaction of **9** with $AgBF_4$ in toluene/benzene produced a much more stable complex $[RuCl(\eta^6\text{-}p\text{-}MeC_6H_4{}^{i}Pr)(L^{4}H)]^{+}BF_4^{-}$ **12**. ^{1}H NMR of a bright orange CD_2Cl_2 solution showed the NH proton once again just above 7 ppm, and the four aromatic CH protons of the $\eta^6\text{-}p\text{-}MeC_6H_4{}^{i}Pr$ ring appearing as four distinct doublets in the region 4.96–6.01 ppm. The aromatic protons of $P(C_6H_5)_2$ also appeared inequivalent, showing the different environments of the two rings as evident in the crystal structure

(see later). In contrast to the apparently conformationally locked primary coordination sphere, the peaks assigned to the protons of the $-(CH_2CH_2)_2CH_2$ ring were broad and ill-defined, possibly indicative of ring fluxionality. The $^{13}C\{^1H\}$ NMR spectrum was assigned fully following analysis of the $^1H-^1H$ COSY and $^1H-^{13}C$ HMQC and HMBC spectra, showing six different environments for the *ortho*-, *meta*- and *para*-carbon atoms, all coupled to ^{31}P to varying degrees. The phosphorus resonance appeared as a singlet at 45.9 ppm in the $^{31}P\{^1H\}$ NMR as expected.

Good elemental analysis of the bulk material was also obtained and the mass spectrum shows only one set of peaks at m/z 555 with the correct isotope pattern for $[M]^+$, furthermore, the high-resolution MS (ES^+) showed the main peak at 555.1280 ($[M]^+$ requires 555.1270).

The X-ray crystal structure of complex 12

On layering a CH_2Cl_2 solution of **12** with pentane, crystals suitable for X-ray crystal analysis were produced. The structure is very similar to that of **10** and so is not shown here (selected bond lengths and angles can be found in Table 4, and details of the structure refinement in Table 2). In particular, bond lengths of the four-membered chelate ring differ by less than 1%. Furthermore, the sum of the internal angles of the heterocyclic ring is 359.6°, indicating that it is essentially planar in geometry. The short P(1)–N(1) bond of 1.658(4) Å combined with the planar nature of the N(1) atom (the sum of the angles around N(1) is 356.7°) is indicative of significant multiple bond character in the P–N bond. The most significant difference to the structure of **10** is in the NH bond length (*ca.* 9% shorter in **12**), however this is presumably due to the fact that the NH in **12** is hydrogen bonded to only one fluorine atom of the BF_4^- counterion ($N(1)\cdots F(1)$ 2.918(4) Å) instead of two in **10**.

The crystal did however, contain some disorder. It was clearly apparent that the thermal parameters of the carbon atoms of one of the phenyl substituents [C(13), C(14), C(16) and C(17), fractional site occupancy = 0.514(15)] were unusually large and this was readily modelled as being due to disorder of this group over two positions related by a rotation about the P–$C\cdots C$(*para*) axis. In addition the refined thermal parameters of some of the C atoms of the *p*-cymene ligand were large and highly anisotropic. This was most satisfactorily modelled over two orientations of the isopropyl group [C(24), C(25) and C(26), fractional site occupancy = 0.687(14)], but neglecting disorder of the phenyl or methyl fragments. The coordinates, anisotropic thermal parameters and site occupancies of the disordered carbon atoms were refined. An attempt was made to solve and refine the structure on the space group *Cc*, however the refinement failed to converge, confirming that the original choice of space group was correct. Attempts to cool the crystal slowly to determine if a less-symmetric ordered structure was preferred at low temperature were frustrated by decomposition of the crystals, presumably as a result of loss of solvent.

Bimetallic complex

Reaction of the complex **6** with 0.5 equivalents of $[\{RuCl(\mu\text{-}Cl)(\eta^6\text{-}p\text{-}MeC_6H_4{}^iPr)\}_2]$ in THF yielded a bimetallic species, $[(\eta^6\text{-}p\text{-}MeC_6H_4{}^iPr)Cl_2Ru(\mu^2,\eta^3\text{-}PPh_2NNMe_2)Ti(C_5H_5)Cl_2]$ **13**, with the two metal centres bridged by the Ph_2PNNMe_2 ligand (Fig. 13). This is the first example of a bimetallic Ru, Ti species bridged by an amino phosphine ligand. The $^{31}P\{^1H\}$ NMR spectrum showed a broad singlet at $\delta = 86.3$ ppm (*cf.* 38.6 ppm for the free ligand, 55.8 in **6** and 65.7 in **7**). The ^1H NMR spectrum showed a downfield shift of the C_5H_5 resonance to 6.51 ppm from 6.19 ppm in **6** and 7.00 ppm in $[(C_5H_5)TiCl_3]$. The aromatic protons of the $\eta^6\text{-}p\text{-}MeC_6H_4{}^iPr$ ligand again appear as two doublets (as for **7**, **8** and **9**), this time at 5.06 and 4.72 ppm with $^3J_{H-H} = 6$ Hz [*cf.* 5.19 and 5.01 ppm, $^3J_{H-H} = 5$ Hz for **7**]. The $^{13}C\{^1H\}$ NMR spectrum shows 10 different carbon environments as expected (the *ipso* carbon resonances could not be detected) with the *ortho*-, *meta*- and *para*- $P(C_6H_5)_2$ carbon atoms appearing as doublets due to coupling to ^{31}P as before. On this occasion, $^{13}C-^{31}P$ coupling is also seen for the aromatic CH carbons of the $\eta^6\text{-}p\text{-}MeC_6H_4{}^iPr$ ligand. The $N(CH_3)_2$ peak is just resolved from the solvent peak (CD_2Cl_2) at 54.2 ppm in the $^{13}C\{^1H\}$ NMR.

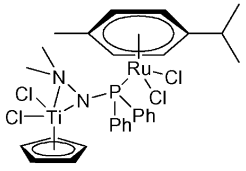

Fig. 13 Structure of bimetallic Ru–Ti complex **13**.

It was not possible to obtain a mass spectrum of the compound despite numerous attempts, due to fragmentation under the mass spectrum conditions. However, the elemental analysis obtained was in excellent agreement with the expected values and the IR spectrum shows peaks at 1436 and 739 cm^{-1} attributed to ν_{P-Ph} and ν_{P-N}, respectively.

Attempts at recrystallization of the orange–brown solid from THF–Et_2O diffusion produced crystals suitable for X-ray analysis. However, the complex decomposes over time in THF producing crystals of the Ru(II) species $[RuCl_2(\eta^6\text{-}p\text{-}MeC_6H_4{}^iPr)(L^2H_2)]^+Cl^-$ (Fig. 14). The structure is very similar to that of **7**, with the main difference being the P(1)–N(1) bond length which is slightly longer at 1.7017(18) Å as opposed to 1.673(3) Å for **7**. The sum of the angles around N(1) is 345.5° (*cf.* 345.9° for **7**) which is considerably flatter than is normal for a secondary amine, and so indicating the possibility of some P–N multiple bonding. The NH groups both participate in hydrogen bond formation. The secondary NH forms a hydrogen bond to a free Cl^- ion ($N(1)\cdots Cl(3)$ 3.1039(19) Å), whereas the tertiary NH group forms a bifurcated intramolecular hydrogen bond to both Cl ligands ($N(2)\cdots Cl(1)$ 3.190(2) and $N(2)\cdots Cl(2)$ 3.138(2) Å).

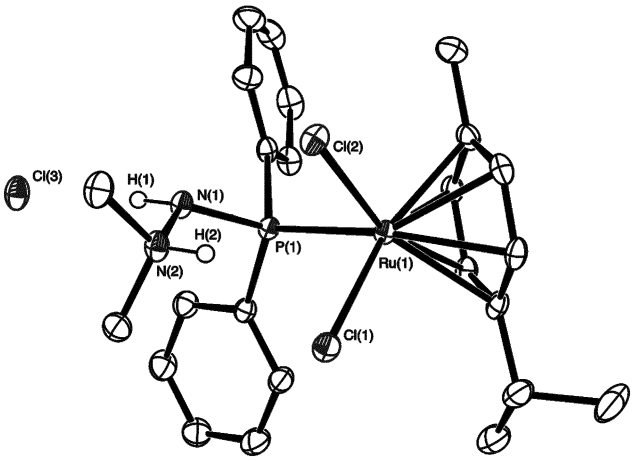

Fig. 14 ORTEP view (40% probability ellipsoids) of the X-ray crystal structure of $[RuCl_2(\eta^6\text{-}p\text{-}MeC_6H_4{}^iPr)(PPh_2NHNHMe_2)]^+Cl^-$ with geometrically positioned hydrogen atoms omitted for clarity.

Conclusions

We have prepared a number of tungsten complexes incorporating the previously unknown phosphazene ligands ($N-PPh_2$). These complexes have unfortunately proved to be unstable so X-ray structure determinations were not possible. DFT calculations, however, showed the P–N ligand to be in a linear arrangement with the nitrogen doubly bonded to the tungsten centre and confirmed that there was no evidence for any multiple bonding between P and N. We have shown that while it is

possible to prepare these M=N–PPh_2 complexes, they are very susceptible to further reactions resulting in the breaking of the P–N bond and the formation of new and unusual ligand types.

Reaction of the same proligand, $Ph_2PN(SiMe_3)_2$, with rhenium resulted in the formation of a new phosphorylketimido ligand complex arising from nucleophilic attack of phosphorus at the nitrile carbon of coordinated acetonitrile.

Reaction of the ligand $Ph_2PNHNMe_2$ with $[(C_5H_5)TiCl_3]$ has produced a complex containing an ionic N,N-bound phosphahydrazido ligand. However, it was not possible to repeat this with the other phosphinohydrazine ligands. In the reaction of these same three ligands with Ru, they acted as simple monodentate phosphines. Formation of new four-membered Ru–P–N–N metal chelates was possible on removal of Cl^- using $AgBF_4$. We also synthesized a Ru–Ti binuclear complex $[(\eta^6\text{-}p\text{-}MeC_6H_4{}^iPr)Cl_2Ru(\mu^2,\eta^3\text{-}PPh_2NNMe_2)Ti(C_5H_5)Cl_2]$ **13**, through reaction of **6** with $[\{RuCl(\mu\text{-}Cl)(\eta^6\text{-}p\text{-}MeC_6H_4{}^iPr)\}_2]$.

The coordination of the phosphorus lone pair to the Ru centre in complexes **7–12** caused a significant (*ca.* 1.5%) reduction in P–N bond length for all the complexes, except **8**, for which there was a 0.01 Å increase in bond length. This increase may help to explain the lower stability of the cationic complex **11** compared to **10** and **12**. The general reduction in bond length is presumably due to an increase in the nitrogen lone pair donation to the phosphorus atom, caused by a reduction in the electron density on the phosphorus on coordination to a metal. This postulate is reinforced by the significantly longer P–N bond length of the Ti(IV) complex, **6** (1.7319(14) Å), due to the reduction in nitrogen lone pair donation to the phosphorus atom on coordination of the nitrogen to the highly Lewis acidic Ti(IV) centre.

Acknowledgements

The authors gratefully acknowledge funding from the EPSRC and would like to thank Johnson Matthey plc for their generous donation of ruthenium starting material and Hermann Starck GmBH for their generous donation of rhenium metal.

References

1 W. A. Nugent and B. L. Haymore, *Coord. Chem. Rev.*, 1980, **31**, 123.
2 J. Chatt and R. L. Richards, *J. Organomet. Chem.*, 1982, **239**, 65.
3 J. R. Dilworth, *Coord. Chem. Rev.*, 1996, **154**, 163.
4 J. Chatt, J. R. Dilworth and R. L. Richards, *Chem. Rev.*, 1978, **78**, 589.
5 V. Ritleng, D. V. Yandulov, W. W. Weare, R. R. Schrock, A. S. Hock and W. M. Davis, *J. Am. Chem. Soc.*, 2004, **126**, 6150.
6 T. Q. Ly, A. M. Z. Slawin and J. D. Woollins, *J. Chem. Soc., Dalton Trans.*, 1997, 1611.
7 S. M. Aucott, A. M. Z. Slawin and J. D. Woollins, *J. Organomet. Chem.*, 1999, **582**, 83.
8 P. A. Bella, O. Crespo, E. J. Fernandez, A. K. Fischer, P. G. Jones, A. Laguna, J. M. Lopez-de-Luzuriaga and M. Monge, *J. Chem. Soc., Dalton Trans.*, 1999, 4009.
9 S. M. Aucott, A. M. Z. Slawin and J. D. Woollins, *J. Chem. Soc., Dalton Trans.*, 2001, 2279.
10 P. Braunstein, B. T. Heaton, C. Jacob, L. Manzi and X. Morise, *Dalton Trans.*, 2003, 1396.
11 F. C. Bradley, E. H. Wong, E. J. Gabe and F. L. Lee, *Inorg. Chim. Acta*, 1986, **120**, L21.
12 H. W. Roesky, H. Voelker, M. Witt and M. Noltemeyer, *Angew. Chem.*, 1990, **102**, 712.
13 J. R. Dilworth, H. J. D. L. Meijer and J. H. Teuben, *J. Organomet. Chem.*, 1978, **159**, 47.
14 I. A. Latham, J. G. Leigh, G. Huttner and I. Jibril, *J. Chem. Soc., Dalton Trans.*, 1986, 337.
15 E. Hollink, J. C. Stewart, P. Wei and D. W. Stephan, *Dalton Trans.*, 2003, 3968.
16 D. W. Stephan, J. C. Stewart, F. Guerin, S. Courtenay, J. Kickham, E. Hollink, C. Beddie, A. Hoskin, T. Graham, P. Wei, P. E. V. H. Spence, W. Xu, L. Koch, X. Gao and D. G. Harrison, *Organometallics*, 2003, **22**, 1937.
17 D. Fenske, B. Maczek and K. Maczek, *Z. Anorg. Allg. Chem.*, 1997, **623**, 1113.
18 T. G. Wetzel, S. Dehnen and P. W. Roesky, *Angew. Chem., Int. Ed.*, 1999, **38**, 1086.
19 O. Kuhl, T. Koch, F. B. Somoza, P. C. Junk, E. Hey-Hawkins, D. Plat and M. S. Eisen, *J. Organomet. Chem.*, 2000, **604**, 116.
20 O. Kuhl, S. Blaurock, J. Sieler and E. Hey-Hawkins, *Polyhedron*, 2001, **20**, 111.
21 O. Schmitz-DuMont and W. Jansen, *Angew. Chem., Int. Ed. Engl.*, 1968, **7**, 382.
22 B. Wrackmeyer, C. Kohler, W. Milius, J. M. Grevy, Z. Garcia-Hernandez and R. Contreras, *Heteroat. Chem.*, 2002, **13**, 667.
23 R. P. Nielsen and H. H. Sisler, *J. Chem. Soc.*, 1962, 3818.
24 H. H. Sisler and R. P. Nielsen, *Inorg. Synth.*, 1966, **8**, 74.
25 R. D. Gorsich, *J. Am. Chem. Soc.*, 1958, **80**, 4744.
26 C. L. Sloan and W. A. Barber, *J. Am. Chem. Soc.*, 1959, **81**, 1364.
27 *GAUSSIAN 98 (Revision A.11.2)*, M. J. Frisch, G. W. Trucks, H. B. Schlegel, G. E. Scuseria, M. A. Robb, J. R. Cheeseman, V. G. Zakrzewski, J. A. Montgomery, R. E. Stratmann, J. C. Burant, S. Dapprich, J. M. Millam, A. D. Daniels, K. N. Kudin, M. C. Strain, O. Farkas, J. Tomasi, V. Barone, M. Cossi, R. Cammi, B. Mennucci, C. Pomelli, C. Adamo, S. Clifford, J. Ochterski, G. A. Petersson, P. Y. Ayala, Q. Cui, K. Morokuma, D. K. Malick, A. D. Rabuck, K. Raghavachari, J. B. Foresman, J. Cioslowski, J. V. Ortiz, B. B. Stefanov, G. Liu, A. Liashenko, P. Piskorz, I. Komaromi, R. Gomperts, R. L. Martin, D. J. Fox, T. Keith, M. A. Al-Laham, C. Y. Peng, A. Nanayakkara, C. Gonzalez, M. Challacombe, P. M. W. Gill, B. G. Johnson, W. Chen, M. W. Wong, J. L. Andres, M. Head-Gordon, E. S. Replogle and J. A. Pople, Gaussian, Inc., Pittsburgh, PA, 1998.
28 A. D. Becke, *J. Chem. Phys.*, 1993, **98**, 5648.
29 R. Ditchfield, W. J. Hehre and J. A. Pople, *J. Chem. Phys.*, 1971, **54**, 724.
30 W. J. Hehre, R. Ditchfield and J. A. Pople, *J. Chem. Phys.*, 1972, **56**, 2257.
31 P. C. Hariharan and J. A. Pople, *Theor. Chim. Acta*, 1973, **28**, 213.
32 P. C. Hariharan and J. A. Pople, *Mol. Phys.*, 1974, **27**, 209.
33 M. S. Gordon, *Chem. Phys. Lett.*, 1980, **76**, 163.
34 R. C. Binning Jr. and L. A. Curtiss, *J. Comput. Chem.*, 1990, **11**, 1206.
35 P. J. Hay and W. R. Wadt, *J. Chem. Phys.*, 1985, **82**, 270.
36 P. J. Hay and W. R. Wadt, *J. Chem. Phys.*, 1985, **82**, 299.
37 W. R. Wadt and P. J. Hay, *J. Chem. Phys.*, 1985, **82**, 284.
38 A. J. H. Wachters, *J. Chem. Phys.*, 1970, **52**, 1033.
39 P. J. Hay, *J. Chem. Phys.*, 1977, **66**, 4377.
40 R. Krishnan, J. S. Binkley, R. Seeger and J. A. Pople, *J. Chem. Phys.*, 1980, **72**, 650.
41 A. D. McLean and G. S. Chandler, *J. Chem. Phys.*, 1980, **72**, 5639.
42 K. Raghavachari and G. W. Trucks, *J. Chem. Phys.*, 1989, **91**, 1062.
43 Z. Otwinowski and W. Minor, Processing of X-ray Diffraction Data Collected in Oscillation Mode, *Methods Enzymol.*, 1997, **276**, 307.
44 A. Altomare, G. Cascarano, G. Giacovazzo, A. Guagliardi, M. C. Burla, G. Polidori and M. Camalli, *J. Appl. Crystallogr.*, 1994, **27**, 435.
45 D. J. Watkin, C. K. Prout, J. R. Carruthers, P. W. Betteridge and R. I. Cooper, *CRYSTALS issue 11*, Chemical Crystallography Laboratory, Oxford, UK, 2001.
46 J. D. Lichtenhan, J. W. Ziller and N. M. Doherty, *Inorg. Chem.*, 1992, **31**, 2893.
47 J. R. Dilworth and S. Morton, *Transition Met. Chem. (London)*, 1987, **12**, 41.
48 J. R. Dilworth, V. C. Gibson, C. Lu, J. R. Miller, C. Redshaw and Y. Zheng, *J. Chem. Soc., Dalton Trans.*, 1997, 269.
49 D. E. C. Corbridge, *Phosphorous: An outline of its Chemistry, Biochemistry and Technology*, Elsevier Science Ltd., Oxford, 4th edn., 1990, p. 47.
50 M. G. B. Drew, D. G. Tisley and R. A. Walton, *J. Chem. Soc. D*, 1970, 600.
51 M. Davis, F. Belanger-Gariepy, D. Zargarian and A. L. Beauchamp, *Acta Crystallogr., Sect. C: Cryst. Struct. Commun.*, 1997, **53**, 428.
52 C. M. P. Ferreira, M. F. C. Guedes da Silva, V. Y. Kukushkin, J. J. R. Frausto da Silva and A. J. L. Pombeiro, *J. Chem. Soc., Dalton Trans.*, 1998, 325.
53 S. Zhang and W. E. Piers, *Organometallics*, 2001, **20**, 2088.
54 A. R. Dias, M. T. Duarte, A. C. Fernandes, S. Fernandes, M. M. Marques, A. M. Martins, J. F. d. Silva and S. S. Rodrigues, *J. Organomet. Chem.*, 2004, **689**, 203.
55 A. L. Spek, *Acta Crystallogr., Sect. C: Cryst. Struct. Commun.*, 1986, **43**, 1233.
56 J. Chatt and G. A. Rowe, *J. Chem. Soc.*, 1962, 4019.
57 J. Chatt, J. D. Garforth, N. P. Johnson and G. A. Rowe, *J. Chem. Soc.*, 1964, 1012.

58 J. Chatt, R. J. Dosser, F. King and G. J. Leigh, *J. Chem. Soc., Dalton Trans.*, 1976, 2435.
59 G. Rouschias and G. Wilkinson, *J. Chem. Soc. A*, 1968, 489.
60 L. R. Falvello, S. Fernández, R. Navarro and E. P. Urriolabeitia, *Inorg. Chem.*, 1997, **36**, 1136.
61 F. A. Cotton, S. A. Duraj, C. C. Hinckley, M. Matusz and W. J. Roth, *Inorg. Chem.*, 1984, **23**, 3080.
62 O. A. Gansow and B. Y. Kimura, *J. Chem. Soc., Chem. Commun.*, 1970, 1621.
63 R. J. Cross, T. H. Green and R. Keat, *J. Chem. Soc., Dalton Trans.*, 1976, 1424.
64 G. E. Graves and L. W. Houk, *J. Inorg. Nuclear Chem.*, 1974, **36**, 232.
65 G. E. Graves and L. W. Houk, *Inorg. Chem.*, 1976, **15**, 7.
66 C. J. Harlan, T. C. Wright, J. L. Atwood and S. G. Bott, *Inorg. Chem.*, 1991, **30**, 1955.
67 H. C. Beachell and S. A. Butter, *Inorg. Chem.*, 1965, **4**, 1133.
68 I. A. Latham, G. J. Leigh, G. Huttner and I. Jibril, *J. Chem. Soc., Dalton Trans.*, 1986, 385.
69 S. M. Aucott, A. M. Z. Slawin and J. D. Woollins, *J. Chem. Soc., Dalton Trans.*, 2000, 2559.
70 T. Q. Ly, A. M. Z. Slawin and J. D. Woollins, *Polyhedron*, 1999, **18**, 1761.
71 Z. Fei, N. Biricik, D. Zhao, R. Scopelliti and P. J. Dyson, *Inorg. Chem.*, 2004, **43**, 2228.
72 S. M. Aucott, A. M. Z. Slawin and J. D. Woollins, *Polyhedron*, 2003, **22**, 361.
73 H. D. Flack and G. Bernardinelli, *J. Appl. Crystallogr.*, 2000, **33**, 1143.
74 A. A. Danopoulos, R. S. Hay-Motherwell, G. Wilkinson, S. M. Cafferkey, T. K. N. Sweet and M. B. Hursthouse, *J. Chem. Soc., Dalton Trans.*, 1997, 3177.